

EUROPEAN ORGANISATION FOR NUCLEAR RESEARCH (CERN)



JHEP06(2016)059
DOI: [10.1007/JHEP06\(2016\)059](https://doi.org/10.1007/JHEP06(2016)059)



CERN-EP-2016-060
17th June 2016

Search for new phenomena in events with a photon and missing transverse momentum in pp collisions at $\sqrt{s} = 13$ TeV with the ATLAS detector

The ATLAS Collaboration

Abstract

Results of a search for new phenomena in events with an energetic photon and large missing transverse momentum with the ATLAS experiment at the Large Hadron Collider are reported. The data were collected in proton–proton collisions at a centre-of-mass energy of 13 TeV and correspond to an integrated luminosity of 3.2 fb^{-1} . The observed data are in agreement with the Standard Model expectations. Exclusion limits are presented in models of new phenomena including pair production of dark matter candidates or large extra spatial dimensions. In a simplified model of dark matter and an axial-vector mediator, the search excludes mediator masses below 710 GeV for dark matter candidate masses below 150 GeV. In an effective theory of dark matter production, values of the suppression scale M_* up to 570 GeV are excluded and the effect of truncation for various coupling values is reported. For the ADD large extra spatial dimension model the search places more stringent limits than earlier searches in the same event topology, excluding M_D up to about 2.3 (2.8) TeV for two (six) additional spatial dimensions; the limits are reduced by 20–40% depending on the number of additional spatial dimensions when applying a truncation procedure.

Contents

1	Introduction	3
2	The ATLAS detector	5
3	Monte Carlo simulation samples	5
4	Event reconstruction	7
5	Event selection	8
6	Background estimation	9
6.1	$Z\gamma$ and $W\gamma$ backgrounds	10
6.2	γ +jets background	10
6.3	Fake photons from misidentified electrons	10
6.4	Fake photons from misidentified jets	11
6.5	Beam-induced background	11
6.6	Final background estimation	11
7	Results	13
8	Systematic uncertainties	14
9	Interpretation of results	15
10	Conclusion	18

1 Introduction

Theories of dark matter (DM) or large extra spatial dimensions (LED) predict the production of events that contain a high transverse momentum (p_T) photon and large missing transverse momentum (referred to as $\gamma + E_T^{\text{miss}}$ events) in pp collisions at a higher rate than is expected in the Standard Model (SM). A sample of $\gamma + E_T^{\text{miss}}$ events with a low expected contribution from SM processes provides powerful sensitivity to models of new phenomena [1–5].

The ATLAS [6, 7] and CMS [8, 9] collaborations have reported limits on various models based on searches for an excess in $\gamma + E_T^{\text{miss}}$ events using pp collisions at centre-of-mass energies of $\sqrt{s} = 7$ and 8 TeV (LHC Run 1). This paper reports the results of a search for new phenomena in $\gamma + E_T^{\text{miss}}$ events in pp collisions at $\sqrt{s} = 13$ TeV.

Although the existence of DM is well established [10], it is not explained by current theories. One candidate is a weakly interacting massive particle (WIMP, also denoted by χ), which has an interaction strength with SM particles near the level of the weak interaction. If WIMPs interact with quarks via a mediator particle, they could be pair-produced in pp collisions at sufficiently high energy. The $\chi\bar{\chi}$ pair would be invisible to the detector, but $\gamma + E_T^{\text{miss}}$ events can be produced via radiation of an initial-state photon in $q\bar{q} \rightarrow \chi\bar{\chi}$ interactions [11].

A model-independent approach to dark matter production in pp collision is through effective field theories (EFT) with various forms of interaction between the WIMPs and the SM particles [11]. However, as the typical momentum transfer in pp collisions at the LHC could reach the cut-off scale required for the EFT approximation to be valid, it is crucial to present the results of the search in terms of models that involve the explicit production of the intermediate state, as shown in Fig. 1 (left). This paper focuses on simplified models assuming Dirac fermion DM candidates produced via an s -channel mediator with axial-vector interactions [12–14]. In this case, the interaction is effectively described by five parameters: the WIMP mass m_χ , the mediator mass m_{med} , the width of the mediator Γ_{med} , the coupling of the mediator to quarks g_q , and the coupling of the mediator to the dark matter particle g_χ . In the limit of large mediator mass, these simplified models map onto the EFT operators, with the suppression scale¹ M_* linked to m_{med} by the relation $M_* = m_{\text{med}}/\sqrt{g_q g_\chi}$ [15].

The paper also considers a specific EFT benchmark, for which neither a simplified model completion nor the simplified models yielding similar kinematic distributions are implemented in an event generator [16]. A dimension-7 EFT operator with direct couplings between DM and electroweak (EW) bosons, and describing a contact interaction of type $\gamma\gamma\chi\bar{\chi}$, is used [14]. The effective coupling to photons is parameterized by the coupling strengths k_1 and k_2 , which control the strength of the coupling to the U(1) and SU(2) gauge sectors of the SM, respectively. In this model, dark matter production proceeds via $q\bar{q} \rightarrow \gamma \rightarrow \gamma\chi\bar{\chi}$, without requiring initial-state radiation. The process is shown in Fig. 1 (right). There are four free parameters in this model: the EW coupling strengths k_1 and k_2 , m_χ , and the suppression scale Λ .

The ADD model of LED [17] aims to solve the hierarchy problem by hypothesizing the existence of n additional spatial dimensions of size R , leading to a new fundamental scale M_D related to the Planck mass, M_{Planck} , through $M_{\text{Planck}}^2 \approx M_D^{2+n} R^n$. If these dimensions are compactified, a series of massive graviton (G) modes results. Stable gravitons would be invisible to the ATLAS detector, but if the graviton

¹ The suppression scale, also referred to as Λ , is the effective mass scale of particles that are integrated out in an EFT. The non-renormalizable operators are suppressed by powers of $1/M_*$.

couples to photons and is produced in association with a photon, the detector signature is a $\gamma + E_T^{\text{miss}}$ event. Examples of graviton production are illustrated in Fig. 2.

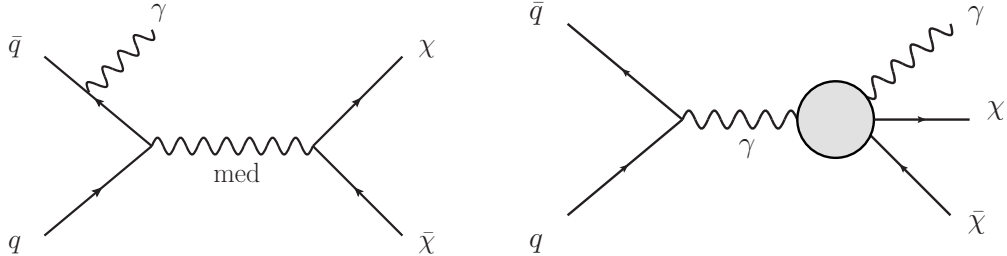


Figure 1: Production of pairs of dark matter particles ($\chi\bar{\chi}$) via an explicit s -channel mediator, med (left) and production of pairs of dark matter particles ($\chi\bar{\chi}$) via an effective $\gamma\gamma\chi\bar{\chi}$ vertex (right).

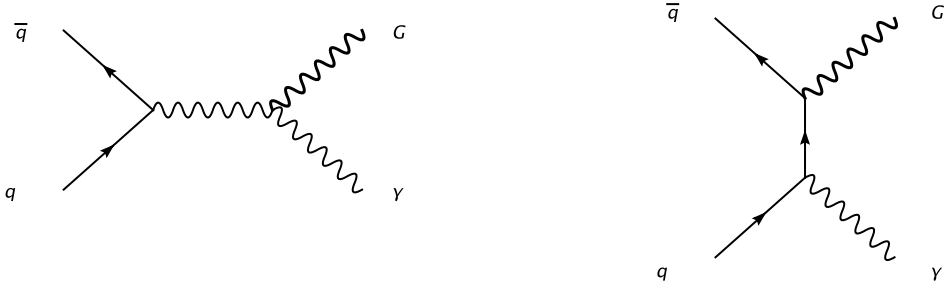


Figure 2: Graviton (G) production in models of large extra dimensions.

The search follows a strategy similar to the search performed using the 8 TeV data collected during the LHC Run 1 [7]. Due to the increased centre-of-mass energy, the search presented here achieves better sensitivity for the ADD model case where direct comparison with the 8 TeV search result is possible, as is shown later. Different DM models, proposed in Ref. [14], are also considered.

The paper is organized as follows. A brief description of the ATLAS detector is given in Section 2. The signal and background Monte Carlo (MC) simulation samples used are described in Section 3. The reconstruction of physics objects is explained in Section 4, and the event selection is described in Section 5. Estimation of the SM backgrounds is outlined in Section 6. The results are described in Section 7 and the systematic uncertainties are given in Section 8. The interpretation of results in terms of models of new phenomena including pair production of dark matter candidates or large extra spatial dimensions is described in Section 9. A summary is given in Section 10.

2 The ATLAS detector

The ATLAS detector [18] is a multi-purpose particle physics apparatus with a forward-backward symmetric cylindrical geometry and near 4π coverage in solid angle.² The inner tracking detector (ID) covers the pseudorapidity range $|\eta| < 2.5$, and consists of a silicon pixel detector, a silicon microstrip detector, and, for $|\eta| < 2.0$, a straw-tube transition radiation tracker (TRT). During the LHC shutdown in 2013–14, an additional inner pixel layer, known as the insertable B-layer [19], was added around a new, smaller radius beam pipe. The ID is surrounded by a thin superconducting solenoid providing a 2 T magnetic field. A high-granularity lead/liquid-argon sampling electromagnetic calorimeter covers the region $|\eta| < 3.2$ and is segmented longitudinally in shower depth. The first layer, with high granularity in the η direction, is designed to allow efficient discrimination between single photon showers and two overlapping photons originating from a π^0 decay. The second layer collects most of the energy deposited in the calorimeter in electromagnetic showers initiated by electrons or photons. Very high energy showers can leave significant energy deposits in the third layer, which can also be used to correct for energy leakage beyond the EM calorimeter. A steel/scintillator-tile calorimeter provides hadronic coverage in the range $|\eta| < 1.7$. The liquid-argon technology is also used for the hadronic calorimeters in the end-cap region $1.5 < |\eta| < 3.2$ and for electromagnetic and hadronic measurements in the forward region up to $|\eta| = 4.9$. The muon spectrometer (MS) surrounds the calorimeters. It consists of three large air-core superconducting toroidal magnet systems, precision tracking chambers providing accurate muon tracking out to $|\eta| = 2.7$, and fast detectors for triggering in the region $|\eta| < 2.4$. A two-level trigger system is used to select events for offline analysis [20].

3 Monte Carlo simulation samples

Several MC simulated samples are used to estimate the signal acceptance, the detector efficiency and to help in the estimation of the SM background contributions.

For all the DM samples considered here, the values of the free parameters and the event generation settings were chosen following the recommendations given in Ref. [14].

Samples of DM production in simplified models are generated via an s -channel mediator with axial-vector interactions. The g_q coupling is set to be universal in quark flavour and equal to 0.25, g_χ is set to 1.0, and Γ_{med} is computed as the minimum width allowed given the couplings and masses. A grid of points in the m_χ – m_{med} plane is generated. The parton distribution function (PDF) set used is NNPDF30_lo_as_0130 [21]. The program MG5_aMC@NLO v2.2.3 [22] is used to generate the events, in conjunction with PYTHIA 8.186 [23] with the NNPDF2.3LO PDF set [24, 25] and the A14 set of tuned parameters (tune) [26]. A photon with at least 130 GeV of transverse momentum is required in MG5_aMC@NLO. For a fixed m_χ , higher m_{med} leads to harder p_T and E_T^{miss} spectra. For a very heavy mediator (≥ 10 TeV), EFT conditions are recovered.

For DM samples from an EFT model involving dimension-7 operators with a contact interaction of type $\gamma\gamma\chi\bar{\chi}$, the parameters which only influence the cross section are set to $k_1 = k_2 = 1.0$ and $\Lambda = 3.0$ TeV. A

² ATLAS uses a right-handed coordinate system with its origin at the nominal interaction point (IP) in the centre of the detector and the z -axis along the beam pipe. The x -axis points from the IP to the centre of the LHC ring, and the y -axis points upward. Cylindrical coordinates (r, ϕ) are used in the transverse plane, ϕ being the azimuthal angle around the beam pipe. The pseudorapidity is defined in terms of the polar θ angle as $\eta = -\ln [\tan(\theta/2)]$.

scan over a range of values of m_χ is performed. The settings of the generators, PDFs, underlying-event tune and generator-level requirements are the same as for the simplified model DM sample generation described above.

Signal samples for ADD models are simulated with the PYTHIA 8.186 generator, using the NNPDF2.3LO PDF with the A14 tune. A requirement of $\hat{p}_{T\min} > 100$ GeV, where $\hat{p}_{T\min}$ defines the lowest transverse momentum used for the generation, is applied to the leading-order (LO) matrix elements for the $2 \rightarrow 2$ process to increase the efficiency of event generation. Simulations are run for two values of the scale parameter M_D (2.0 and 3.0 TeV) and with the number of extra dimensions, n , varied from two to six.

For $W/Z\gamma$ backgrounds, events containing a charged lepton and neutrino or a lepton pair (lepton is an e , μ or τ), together with a photon and associated jets are simulated using the SHERPA 2.1.1 generator [27]. The matrix elements including all diagrams with three electroweak couplings are calculated with up to three partons at LO and merged with SHERPA parton shower [28] using the ME+PS@LO prescription [29]. The CT10 PDF set [30] is used in conjunction with a dedicated parton shower tuning developed by the SHERPA authors. For γ^*/Z events with the Z decaying to charged particles a requirement on the dilepton invariant mass of $m_{\ell\ell} > 10$ GeV is applied at generator level.

Events containing a photon with associated jets are also simulated using SHERPA 2.1.1, generated in several bins of photon p_T from 35 GeV up to larger than 4 TeV. The matrix elements are calculated at LO with up to three partons (lowest p_T slice) or four partons and merged with SHERPA parton shower using the ME+PS@LO prescription. The CT10 PDF set is used in conjunction with the dedicated parton shower tuning.

For $W/Z+\text{jets}$ backgrounds, events containing W or Z bosons with associated jets are again simulated using SHERPA 2.1.1. The matrix elements are calculated for up to two partons at NLO and four partons at LO using the Comix [31] and OpenLoops [32] matrix element generators and merged with SHERPA parton shower using the ME+PS@NLO prescription [33]. As in the case of the $\gamma+\text{jets}$ samples, the CT10 PDF set is used together with the dedicated parton shower tuning. The $W/Z+\text{jets}$ events are normalized to NNLO cross sections [34]. These samples are also generated in several p_T bins.

Multi-jet processes are simulated using the PYTHIA 8.186 generator. The A14 tune is used together with the NNPDF2.3LO PDF set. The EvtGen v1.2.0 program [35] is used to simulate the bottom and charm hadron decays.

Diboson processes with four charged leptons, three charged leptons and one neutrino or two charged leptons and two neutrinos are simulated using the SHERPA 2.1.1 generator. The matrix elements contain all diagrams with four electroweak vertices. They are calculated for up to one parton (for either four charged leptons or two charged leptons and two neutrinos) or zero partons (for three charged leptons and one neutrino) at NLO, and up to three partons at LO using the Comix and OpenLoops matrix element generators and merged with SHERPA parton shower using the ME+PS@NLO prescription. The CT10 PDF set is used in conjunction with the dedicated parton shower tuning. The generator cross sections are used in this case, which are at NLO.

For the generation of $t\bar{t}$ and single top quarks in the Wt and s -channel, the PowHEG-Box v2 [36, 37] generator is used, with the CT10 PDF set used in the matrix element calculations. For all top processes, top-quark spin correlations are preserved. For t -channel production, top quarks are decayed using MadSpin [38]. The parton shower, fragmentation, and the underlying event are simulated using PYTHIA 6.428 [39] with the CTEQ6L1 [40] PDF sets and the corresponding Perugia 2012 tune [41]. The

top mass is set to 172.5 GeV. The EvtGen v1.2.0 program is used for properties of the bottom and charm hadron decays.

Multiple $p\bar{p}$ interactions in the same or neighbouring bunch crossings superimposed on the hard physics process (referred to as pile-up) are simulated with the soft QCD processes of PYTHIA 8.186 using the A2 tune [42] and the MSTW2008LO PDF set [43]. The events are reweighted to accurately reproduce the average number of interactions per bunch crossing in data.

All simulated samples are processed with a full ATLAS detector simulation [44] based on GEANT4 [45]. The simulated events are reconstructed and analysed with the same analysis chain as for the data, using the same trigger and event selection criteria discussed in Section 5.

4 Event reconstruction

Photons are reconstructed from clusters of energy deposits in the electromagnetic calorimeter measured in projective towers. Clusters without matching tracks are classified as unconverted photon candidates. A photon is considered as a converted photon candidate if it is matched to a pair of tracks that pass a requirement on TRT-hits [46] and form a vertex in the ID which is consistent with originating from a massless particle, or if it is matched to a single track passing a TRT-hits requirement and has a first hit after the innermost layer of the pixel detector. The photon energy is corrected by applying the energy scales measured with $Z \rightarrow e^+e^-$ decays [47]. The trajectory of the photon is reconstructed using the longitudinal (shower depth) segmentation of the calorimeters and a constraint from the average collision point of the proton beams. For converted photons, the position of the conversion vertex is also used if tracks from the conversion have hits in the silicon detectors. Identification requirements are applied in order to reduce the contamination from π^0 or other neutral hadrons decaying to two photons. The photon identification is based on the profile of the energy deposits in the first and second layers of the electromagnetic calorimeter. Candidate photons are required to have $p_T > 10$ GeV, to satisfy the "loose" identification criteria defined in Ref. [48] and to be within $|\eta| < 2.37$. Photons used in the event selection must additionally satisfy the "tight" identification criteria [48] and be isolated as follows. The energy in the calorimeters in a cone of size $\Delta R = \sqrt{(\Delta\eta)^2 + (\Delta\phi)^2} = 0.4$ around the cluster barycentre excluding the energy associated with the photon cluster is required to be less than $2.45 \text{ GeV} + 0.022 p_T^\gamma$, where p_T^γ is the p_T of the photon candidate. This cone energy is corrected for the leakage of the photon energy from the central core and for the effects of pile-up [47].

Electrons are reconstructed from clusters in the electromagnetic calorimeter matched to a track in the ID. The criteria for their identification, and the calibration steps, are similar to those used for photons. Electron candidates must satisfy the "medium" identification requirement of Ref. [47]. Muons are identified either as a combined track in the MS and ID systems, or as an ID track that, once extrapolated to the MS, is associated with at least one track segment in the MS. Muon candidates must satisfy the "medium" identification requirement [49]. The significance of the transverse impact parameter, defined as the transverse impact parameter d_0 divided by its estimated uncertainty, σ_{d_0} , of tracks with respect to the primary vertex³ is required to satisfy $|d_0|/\sigma_{d_0} < 5.0$ for electrons and $|d_0|/\sigma_{d_0} < 3.0$ for muons. The longitudinal impact parameter z_0 must be $|z_0| \sin \theta < 0.5$ mm for both electrons and muons. Electrons are required to have $p_T > 7$ GeV and $|\eta| < 2.47$, while muons are required to have $p_T > 6$ GeV and $|\eta| < 2.7$.

³ The primary vertex is defined as the vertex with the highest sum of the squared transverse momenta of its associated tracks. It is reconstructed from at least two associated tracks with $p_T > 0.4$ GeV.

If any selected electron shares its inner detector track with a selected muon, the electron is removed and the muon is kept, in order to remove electron candidates coming from muon bremsstrahlung followed by photon conversion.

Jets are reconstructed using the anti- k_t algorithm [50, 51] with a radius parameter $R = 0.4$ from clusters of energy deposits at the electromagnetic scale in the calorimeters. A correction used to calibrate the jet energy to the scale of its constituent particles [52, 53] is then applied. In addition, jets are corrected for contributions from pile-up interactions [52]. Candidate jets are required to have $p_T > 20$ GeV. To suppress pile-up jets, which are mainly at low p_T , a jet vertex tagger [54], based on tracking and vertexing information, is applied in jets with $p_T < 50$ GeV and $|\eta| < 2.4$. Jets used in the event selection are required to have $p_T > 30$ GeV and $|\eta| < 4.5$. Hadronically decaying τ leptons are considered as jets as in the Run 1 analysis [7].

To resolve ambiguities which can happen in object reconstruction, an overlap removal procedure is performed in the following order. If an electron lies within $\Delta R < 0.2$ of a candidate jet, the jet is removed from the event, while if an electron lies within $0.2 < \Delta R < 0.4$ of a jet, the electron is removed. Muons lying within $\Delta R < 0.4$ with respect to the remaining candidate jets are removed, except if the number of tracks with $p_T > 0.5$ GeV associated with the jet is less than three. In the latter case, the jet is discarded and the muon kept. Finally if a candidate photon lies within $\Delta R < 0.4$ of a jet, the jet is removed.

The momentum imbalance in the transverse plane is obtained from the negative vector sum of the reconstructed and calibrated physics objects, selected as described above, and is referred to as missing transverse momentum, E_T^{miss} . The symbol E_T^{miss} is used to denote its magnitude. Calorimeter energy deposits and tracks are associated with a reconstructed and identified high- p_T object in a specific order: electrons with $p_T > 7$ GeV, photons with $p_T > 10$ GeV, and jets with $p_T > 20$ GeV [55]. Tracks from the primary vertex not associated with any such objects ("soft term") are also taken into account in the E_T^{miss} reconstruction [56]. This track-based soft term is more robust against pile-up and provides a better E_T^{miss} measurement in terms of resolution and scale than the calorimeter-based soft term used in Ref. [7].

Corrections are applied to the objects in the simulated samples to account for differences compared to data in object reconstruction, identification and isolation efficiencies for both the selected leptons and photons and for the vetoed leptons.

5 Event selection

The data were collected in pp collisions at $\sqrt{s} = 13$ TeV during 2015. The events for the analysis are recorded using a trigger requiring at least one photon candidate with an online p_T threshold of 120 GeV passing "loose" identification requirements based on the shower shapes in the EM calorimeter as well as on the energy leaking into the hadronic calorimeter from the EM calorimeter [57]. Only data satisfying beam, detector and data quality criteria are considered. The data used for the analysis correspond to an integrated luminosity of 3.2 fb^{-1} . The uncertainty in the integrated luminosity is $\pm 5\%$. It is derived following a methodology similar to that detailed in Ref. [58], from a preliminary calibration of the luminosity scale using $x-y$ beam-separation scans performed in August 2015.

Quality requirements are applied to photon candidates in order to reject events containing photons arising from instrumental problems or from non-collision background [46]. Beam-induced background is highly suppressed by applying the criteria described in Section 6.5. In addition, quality requirements are applied to remove events containing candidate jets arising from detector noise and out-of-time energy deposits

in the calorimeter from cosmic rays or other non-collision sources [59]. Events are required to have a reconstructed primary vertex.

The criteria for selecting events in the signal region (SR) are optimized considering the discovery potential for the simplified dark matter model. This SR also provides good sensitivity to the other models described in Section 1. Events in the SR are required to have $E_T^{\text{miss}} > 150 \text{ GeV}$ and the leading photon has to satisfy the "tight" identification criteria, to have $p_T^\gamma > 150 \text{ GeV}$, $|\eta| < 2.37$, excluding the calorimeter barrel/end-cap transition region $1.37 < |\eta| < 1.52$, and to be isolated. With respect to the Run 1 analysis, a re-optimization was performed that leaded to the following changes: a higher threshold for p_T^γ (150 GeV instead of 125 GeV) and a larger $|\eta|$ region ($|\eta| < 2.37$ instead of 1.37) are used for the leading photon. It is required that the photon and E_T^{miss} do not overlap in the azimuth: $\Delta\phi(\gamma, E_T^{\text{miss}}) > 0.4$. Events with more than one jet or with a jet with $\Delta\phi(\text{jet}, E_T^{\text{miss}}) < 0.4$ are rejected. The remaining events with one jet are retained to increase the signal acceptance and reduce systematic uncertainties related to the modelling of initial-state radiation. Events are required to have no electrons or muons passing the requirements described in Section 4. The lepton veto mainly rejects W/Z events with charged leptons in the final state. For events satisfying these criteria, the efficiency of the trigger used in the analysis is $0.997^{+0.003}_{-0.008}$, as determined using a control sample of events selected with a E_T^{miss} trigger with a threshold of 70 GeV.

The final data sample contains 264 events, of which 80 have a converted photon, and 170 and 94 events have zero and one jet, respectively.

The total number of events observed in the SR in data is compared with the estimated total number of events in the SR from SM backgrounds. The latter is obtained from a simultaneous fit to various control regions (CR) defined in the following. Single-bin SR and CRs are considered in the fit: no shape information within these regions is used.

6 Background estimation

The SM background to the $\gamma + E_T^{\text{miss}}$ final state is dominated by the $Z(\rightarrow \nu\nu)\gamma$ process, where the photon is due to initial-state radiation. Secondary contributions come from $W\gamma$ and $Z\gamma$ production with unidentified electrons, muons or with hadronically decaying τ leptons. There is also a contribution from W/Z production where a lepton or an associated radiated jet is misidentified as a photon. In addition, there are smaller contributions from top-quark pair, diboson, $\gamma+\text{jets}$ and multi-jet production.

All background estimations are extrapolated from orthogonal data samples. Control regions, built to be enriched in a specific background, are used to constrain the normalization of $W/Z\gamma$ and $\gamma+\text{jets}$ backgrounds. The normalization is obtained via a simultaneous likelihood fit [60] to the observed yields in all single-bin CRs. Poisson likelihood functions are used to model the expected event yields in all regions. The systematic uncertainties described in Section 8 are treated as Gaussian-distributed nuisance parameters in the likelihood function. The fit in the CRs is performed to obtain the normalization factors for the $W\gamma$, $Z\gamma$ and $\gamma+\text{jets}$ processes, which are then used to constrain background estimates in the SR. The same normalization factor is used for both $Z(\rightarrow \nu\nu)\gamma$ and Z decaying to charged leptons in SR events.

The backgrounds due to fake photons from the misidentification of electrons or jets in $W/Z+\text{jets}$, top, diboson and multi-jet events are estimated using data-driven techniques based on studies of electrons and jets faking photons (see Sections 6.3 and 6.4).

6.1 $Z\gamma$ and $W\gamma$ backgrounds

For the estimation of the $W/Z\gamma$ background, three control regions are defined by selecting events with the same criteria used for the SR but inverting the lepton vetoes. In the first control region (1muCR) the $W\gamma$ contribution is enhanced by requiring the presence of a muon. The second and third control regions enhance the $Z\gamma$ background by requiring the presence of a pair of muons (2muCR) or electrons (2eleCR). In both 1muCR and 2muCR, to ensure that the E_T^{miss} spectrum is similar to the one in the SR, muons are treated as non-interacting particles in the E_T^{miss} reconstruction. The same procedure is followed for electrons in the 2eleCR. In each case, the CR lepton selection follows the same requirements as the SR lepton veto, with the addition that the leptons must be isolated with "loose" criteria [49]. In both the $Z\gamma$ -enriched control regions, the dilepton invariant mass $m_{\ell\ell}$ is required to be greater than 20 GeV. The normalization of the dominant $Z\gamma$ background process is largely constrained by the event yields in the 2muCR and the 2eleCR. The signal contamination in all CRs is negligible. The expected fraction of signal events in the 1muCR is at the level of 0.15%. In the 2muCR and 2eleCR the contamination is zero due to the requirement of two leptons.

6.2 $\gamma+\text{jets}$ background

The $\gamma+\text{jets}$ background in the signal region consists of events where the jet is poorly reconstructed and partially lost, creating fake E_T^{miss} . This background is suppressed by the large E_T^{miss} and the large jet– E_T^{miss} azimuthal separation requirements. It is estimated from simulated $\gamma+\text{jets}$ events corrected with a normalization factor that is determined in a specific control region (PhJetCR), enriched in $\gamma+\text{jets}$ events. This CR is defined with the same criteria as used for the SR, but requiring $85 \text{ GeV} < E_T^{\text{miss}} < 110 \text{ GeV}$ and azimuthal separation between the photon and E_T^{miss} , $\Delta\phi(\gamma, E_T^{\text{miss}})$, to be smaller than 3, to minimize the contamination from signal events. The upper limit on the expected fraction of signal events in the PhJetCR has been estimated to be at the level of 3%. The extrapolation in E_T^{miss} of the gamma+jets background from the CR to the SR was checked in a validation region defined with higher E_T^{miss} ($125 < E_T^{\text{miss}} < 250 \text{ GeV}$) and requiring $\Delta\phi(\gamma, E_T^{\text{miss}}) < 3.0$; no evidence of mismodeling was found.

6.3 Fake photons from misidentified electrons

Contributions from processes in which an electron is misidentified as a photon are estimated by scaling yields from a sample of $e + E_T^{\text{miss}}$ events by an electron-to-photon misidentification factor. This factor is measured with mutually exclusive samples of e^+e^- and $\gamma + e$ events in data. To establish a pure sample of electrons, m_{ee} and m_{ey} are both required to be consistent with the Z boson mass to within 10 GeV, and the E_T^{miss} is required to be smaller than 40 GeV. The misidentification factor, calculated as the ratio of the number of $\gamma + e$ to the number of e^+e^- events, is parameterized as a function of p_T and pseudorapidity and it varies between 0.8% and 2.6%. Systematic uncertainties from three different sources are added in quadrature: the difference between misidentification factors measured in data in two different windows around the Z mass (5 GeV and 10 GeV), the difference when measured in $Z(\rightarrow ee)$ MC events with the same method as used in data compared to using generator-level information, and the difference when measured in $Z(\rightarrow ee)$ and $W(\rightarrow ev)$ MC events using generator-level information. Similar estimates are made for the three control regions with leptons, by applying the misidentification factor to events selected using the same criteria as used for these control regions but requiring an electron instead of a photon. The estimated contribution of this background in the SR and the associated error are reported in Section 7.

6.4 Fake photons from misidentified jets

Background contributions from events in which a jet is misidentified as a photon are estimated using a sideband counting method [61]. This method relies on counting photon candidates in four regions of a two-dimensional space, defined by the transverse isolation energy and by the quality of the identification criteria. A signal region (region A) is defined by photon candidates that are isolated with tight identification. Three background regions are defined, consisting of photon candidates which are either tight and non-isolated (region B), non-tight and isolated (region C) or non-tight and non-isolated (region D). The method relies on the fact that signal contamination in the three background regions is small and that the isolation profile in the non-tight region is the same as that of the background in the tight region. The number of background candidates in the signal region (N_A) is calculated by taking the ratio of the two non-tight regions (N_C/N_D) multiplied by the number of candidates in the tight, non-isolated region (N_B). This method is applied in all analysis regions: the SR and the four CRs. The systematic uncertainty of the method is evaluated by varying the criteria of tightness and isolation used to define the four regions. This estimate also accounts for the contribution from multi-jet events, which can mimic the $\gamma + E_T^{\text{miss}}$ signature if one jet is misreconstructed as a photon and one or more of the other jets are poorly reconstructed, resulting in large E_T^{miss} . The estimated contribution of this background in the SR and the associated error are reported in Section 7.

6.5 Beam-induced background

Muons from beam background can leave significant energy deposits in the calorimeters, mainly in the region at large $|\eta|$, and hence can lead to reconstructed fake photons. These beam-induced fakes do not point back to the primary vertex, and the photon trajectory provides a powerful rejection criterion. The $|z|$ position of the intersection of the extrapolated photon trajectory with the beam axis is required to be smaller than 0.25 m, which rejects 98.5% of these fake photons. The residual beam background after the final event selection is found to be negligible, about 0.02%.

6.6 Final background estimation

Background estimates in the SR are derived from a simultaneous fit to the four single-bin control regions (1muCR, 2muCR, 2eleCR and PhJetCR) in order to assess whether the observed SR yield is consistent with the background model. For each CR, the inputs to the fit are: the number of events seen in the data, the number of events expected from MC simulation for the W/γ and $\gamma+\text{jets}$ backgrounds, whose normalizations are free parameters, and the number of fake-photon events obtained from the data-driven techniques. The fitted values of the normalization factors for $W\gamma$ and $Z\gamma$ are $k_{W\gamma} = 1.50 \pm 0.26$ and $k_{Z\gamma} = 1.19 \pm 0.21$, while the normalization factor for the $\gamma+\text{jets}$ background is $k_{\gamma+\text{jets}} = 0.98 \pm 0.28$. The uncertainties include those from the various sources described in Section 8. The factor $k_{W\gamma}$ is large owing to the data–MC normalization difference in the 1muCR, which can potentially be reduced using higher-order corrections for the $V\gamma$ cross sections [62], which are not available for the selection criteria used here.

Post-fit distributions of E_T^{miss} in the three lepton CRs and in the PhJetCR are shown in Fig. 3 and Fig. 4. These distributions illustrate the kinematics of the selected events. Their shape is not used in the simultaneous fit, which is performed on the single-bin CRs.

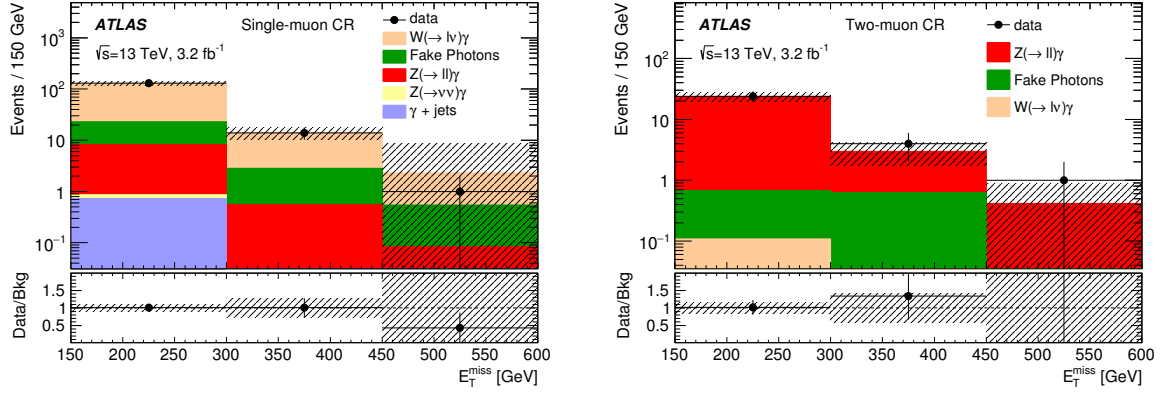


Figure 3: Distribution of E_T^{miss} , reconstructed treating muons as non-interacting particles, in the data and for the background in the 1muCR (left) and in the 2muCR (right). The total background expectation is normalized to the post-fit result in each control region. Overflows are included in the final bin. The error bars are statistical, and the dashed band includes statistical and systematic uncertainties determined by a bin-by-bin fit. The lower panel shows the ratio of data to expected background event yields.

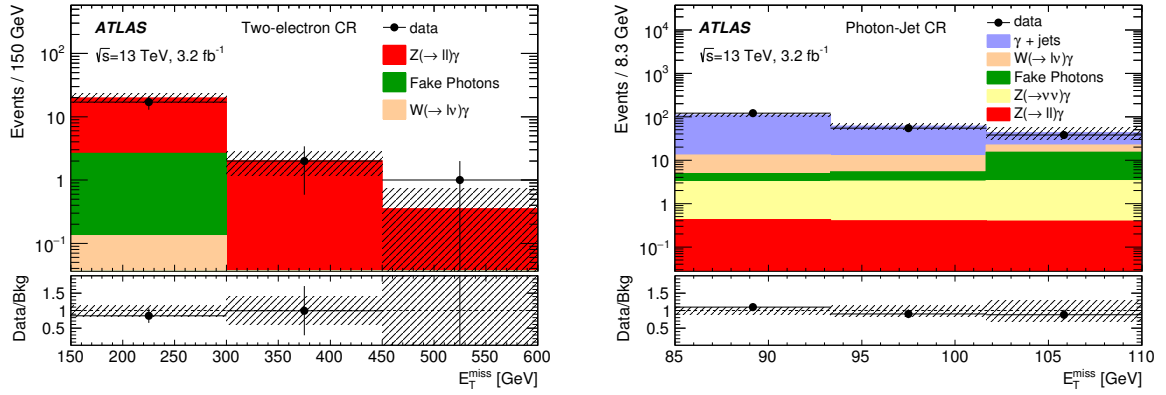


Figure 4: Distribution of E_T^{miss} in the data and for the background in the 2eleCR, where E_T^{miss} is reconstructed treating electrons as non-interacting particles (left) and in the PhJetCR (right). The total background expectation is normalized to the post-fit result in each control region. Overflows are included in the final bin for the left figure. The error bars are statistical, and the dashed band includes statistical and systematic uncertainties determined by a bin-by-bin fit. The lower panel shows the ratio of data to expected background event yields.

7 Results

Table 1 presents the observed number of events and the SM background predictions in the SR, obtained from the simultaneous fit to the single-bin CRs. The same numbers are also shown in the three lepton CRs and in the PhJetCR. The contribution from $W/Z\gamma$ with W/Z decaying to τ includes both the leptonic and the hadronic τ decays, considered in this search as jets. The fraction of $W(\rightarrow \tau\nu)$ and $Z(\rightarrow \tau\tau)$ with respect to the total background corresponds to about 12% and 0.8%, respectively. The post-fit E_T^{miss} distribution and the photon p_T distribution in the SR are shown in Fig. 5.

Table 1: Observed event yields in 3.2 fb^{-1} compared to expected yields from SM backgrounds in the signal region (SR) and in the four control regions (CRs), as predicted from the simultaneous fit to all single-bin CRs. The MC yields before the fit are also shown. The uncertainty includes both the statistical and systematic uncertainties described in Section 8. The individual uncertainties can be correlated and do not necessarily add in quadrature to equal the total background uncertainty.

	SR	1muCR	2muCR	2eleCR	PhJetCR
Observed events	264	145	29	20	214
Fitted Background	295 ± 34	145 ± 12	27 ± 4	23 ± 3	214 ± 15
$Z(\rightarrow \nu\nu)\gamma$	171 ± 29	0.15 ± 0.03	0.00 ± 0.00	0.00 ± 0.00	8.6 ± 1.4
$W(\rightarrow \ell\nu)\gamma$	58 ± 9	119 ± 17	0.14 ± 0.04	0.11 ± 0.03	22 ± 4
$Z(\rightarrow \ell\ell)\gamma$	3.3 ± 0.6	7.9 ± 1.3	26 ± 4	20 ± 3	1.2 ± 0.2
$\gamma + \text{jets}$	15 ± 4	0.7 ± 0.5	0.00 ± 0.00	0.03 ± 0.03	166 ± 17
Fake photons from electrons	22 ± 18	1.7 ± 1.5	0.05 ± 0.05	0.00 ± 0.00	5.8 ± 5.1
Fake photons from jets	26 ± 12	16 ± 11	1.1 ± 0.8	2.5 ± 1.3	9.9 ± 3.1
Pre-fit background	249 ± 29	105 ± 14	23 ± 2	19 ± 2	209 ± 50

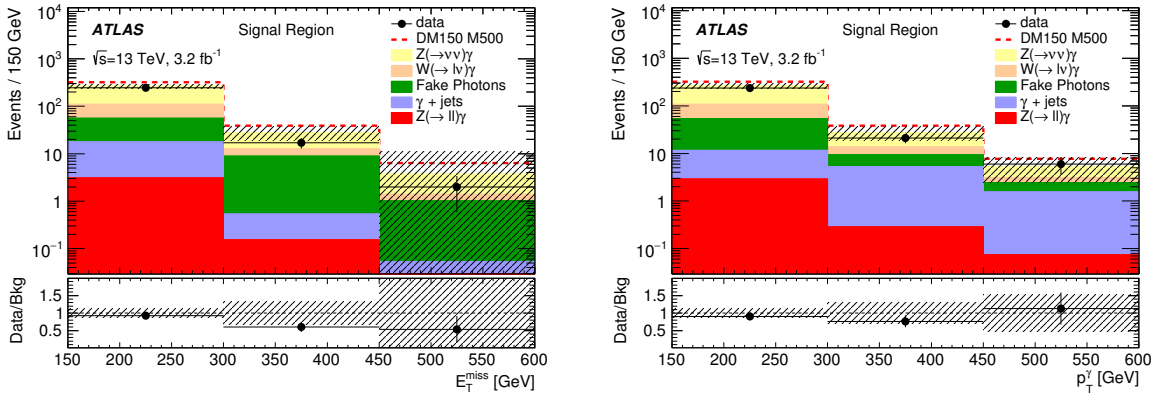


Figure 5: Distribution of E_T^{miss} (left) and photon p_T (right) in the signal region for data and for the background predicted from the fit in the CRs. Overflows are included in the final bin. The error bars are statistical, and the dashed band includes statistical and systematic uncertainties determined by a bin-by-bin fit. The expected yield of events from the simplified model with $m_\chi = 150 \text{ GeV}$ and $m_{\text{med}} = 500 \text{ GeV}$ is stacked on top of the background prediction. The lower panel shows the ratio of data to expected background event yields.

8 Systematic uncertainties

Systematic uncertainties in the background predictions in the SR are presented as percentages of the total background prediction. This prediction is obtained from the simultaneous fit to all single-bin CRs, which provides constraints on many sources of systematic uncertainty, as the normalizations of the dominant background processes are fitted parameters. The dominant systematic uncertainties are summarised in Table 2.

The total background prediction uncertainty, including systematic and statistical contributions, is approximately 11%, dominated by the statistical uncertainty in the control regions, which amounts to approximately 9%. The largest relative systematic uncertainty of 5.8% is due to the electron fake rate. This is mainly driven by the small number of events available for the estimation of the electron-to-photon misidentification factor yielding a precision of 30–100%, depending on p_T and η . PDF uncertainties have an impact on the $V\gamma$ samples in each region but the effect on normalization is largely absorbed in the fit. They are evaluated following the prescriptions of the PDF group recommendations [63] and using a reweighting procedure implemented in the LHAPDF Tool [64]. These uncertainties contribute 2.8% to the background prediction uncertainty affecting mainly the $Z(\rightarrow v\nu)\gamma$ background. The uncertainty on the jet fake rate contributes a relative uncertainty of 2.4% and affects mainly the normalization of $W(\rightarrow \ell\nu)\gamma$ background, while the uncertainty on the muon reconstruction and isolation efficiency gives a relative uncertainty of 1.5% and mainly affects the $Z(\rightarrow \ell\ell)\gamma$ background. Finally the uncertainty on the jet energy resolution accounts for 1.2% of the uncertainty and the most affected background is $\gamma + \text{jets}$. After the fit, the uncertainty on the luminosity [58] is found to have a negligible impact on the background estimation.

For the signal-related systematics, the PDF uncertainties are evaluated in the same way described above for the background samples, while QCD scale uncertainties are evaluated by varying the renormalization and factorization scales by factors 2.0 and 0.5 with respect to the nominal values used in the MC generation. The uncertainties due to the choice of underlying-event tune used with PYTHIA 8.186 are computed by generating MC samples with the alternative underlying-event tunes described in Ref. [26].

Table 2: Breakdown of the dominant systematic uncertainties in the background estimates. The uncertainties are given relative to the expected total background yield. The individual uncertainties can be correlated and do not necessarily add in quadrature to equal the total background uncertainty.

Total background	295
Total background uncertainty	11%
Electron fake rate	5.8%
PDF uncertainties	2.8%
Jet fake rate	2.4%
Muons reconstruction/isolation efficiency	1.5%
Electrons reconstruction/identification/isolation efficiency	1.3%
Jet energy resolution [65]	1.2%
Photon energy scale	0.6%
E_T^{miss} soft term scale and resolution	0.4%
Photon energy resolution	0.2%
Jet energy scale [53]	0.1%

9 Interpretation of results

The 264 events observed in data are consistent with the prediction of 295 ± 34 events from SM backgrounds. The results are therefore interpreted in terms of exclusion limits in models that would produce an excess of $\gamma + E_T^{\text{miss}}$ events. Upper bounds are calculated using a one-sided profile likelihood ratio and the CL_S technique [66, 67], evaluated using the asymptotic approximation [68]. The likelihood fit includes both the SR and the CRs.

Limits on the fiducial cross section of a potential signal beyond the SM, defined as the product of the cross section times the fiducial acceptance A , are provided. These limits can be extrapolated within some approximations to models producing $\gamma + E_T^{\text{miss}}$ events once A is known. The value of A for a particular model is computed by applying the same selection criteria as in the SR but at the particle level; in this computation E_T^{miss} is given by the vector sum of the transverse momenta of all invisible particles. The value of A is 0.43–0.56 (0.4) for the DM (ADD) samples generated for this search following the specifications given in Section 3. The limit is computed by dividing the limit on the visible cross section $\sigma \times A \times \epsilon$ by the fiducial reconstruction efficiency ϵ . The latter is conservatively taken to be 78%, corresponding to the lowest efficiency found in the ADD and DM models studied here, for which the efficiency ranges from 78% to 91%. The observed (expected) upper limits on the fiducial cross section $\sigma \times A$ for the production of $\gamma + E_T^{\text{miss}}$ events are 17.8 (25.5) fb at 95% confidence level (CL) and 14.6 (21.7) fb at 90% CL. The observed upper limit at 95% CL would be 15.3 fb using the largest efficiency value of 91%.

When placing limits on specific models, the signal-related systematic uncertainties calculated as described in Section 8 affecting $A \times \epsilon$ (PDF, scales, initial- and final-state radiation) are included in the statistical analysis, while the uncertainties affecting the cross section (PDF, scales) are indicated as bands around the observed limits and written as σ_{theo} .

Simplified models with explicit mediators are robust for all values of the momentum transfer Q_{tr} [14]. For the simplified model with an axial-vector mediator, Fig. 6 shows the observed and expected contours corresponding to a 95% CL exclusion as a function of m_{med} and m_χ for $g_q = 0.25$ and $g_\chi = 1$. The region of the plane under the limit curves is excluded. The region not allowed due to perturbative unitarity violation is to the left of the line defined by $m_\chi = \sqrt{\pi/2}m_{\text{med}}$ [69]. The line corresponding to the DM thermal relic abundance [70] is also indicated in the figure. The search excludes mediator masses below 710 GeV for χ masses below 150 GeV.

Figure 7 shows the contour corresponding to a 90% CL exclusion translated to the χ -proton scattering cross section vs. m_χ plane. Bounds on the χ -proton cross section are obtained following the procedure described in Ref. [71], assuming that the axial-vector mediator with couplings $g_q = 0.25$ and $g_\chi = 1.0$ is solely responsible for both collider χ pair production and for χ -nucleon scattering. In this plane a comparison with the result from direct DM searches [72–74] is possible. The search provides stringent limits on the scattering cross section at the order of 10^{-41} cm^2 up to m_χ masses of about 150 GeV. The limit placed in this search extends to arbitrarily low values of m_χ , as the acceptance at lower mass values is the same as the one at the lowest m_χ value shown here.

In the case of the model of $\gamma\gamma\chi\bar{\chi}$ interactions, lower limits are placed on the effective mass scale M_* as a function of m_χ , as shown in Fig. 8. The EFT is not always valid, so a truncation procedure is applied [75]. In this procedure, the scale at which the EFT description becomes invalid (M_{cut}) is assumed to be related to M_* through $M_{\text{cut}} = g^* M_*$, where g^* is the EFT coupling. Events having a centre-of-mass energy larger than M_{cut} are removed and the limit is recomputed. The effect of the truncation for various representative

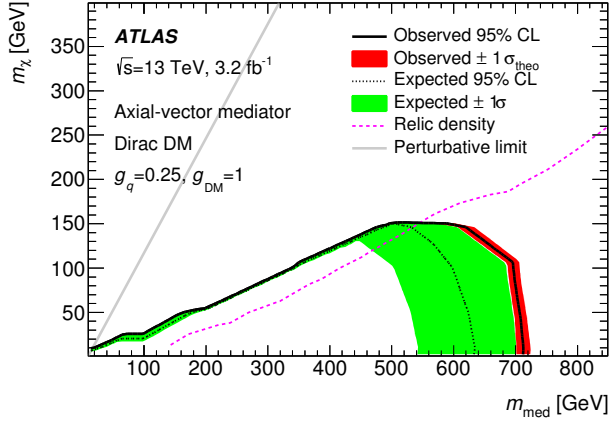


Figure 6: The observed and expected 95% CL exclusion limit for a simplified model of dark matter production involving an axial-vector operator, Dirac DM and couplings $g_q = 0.25$ and $g_\chi = 1$ as a function of the dark matter mass m_χ and the axial-mediator mass m_{med} . The plane under the limit curves is excluded. The region on the left is excluded by the perturbative limit. The relic density curve [70] is also shown.

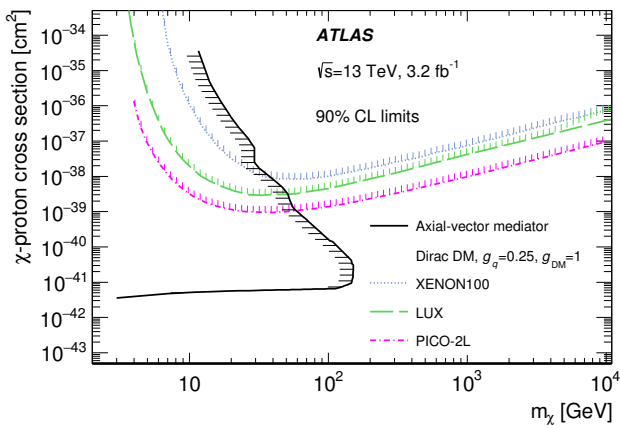


Figure 7: The 90% CL exclusion limit on the χ -proton scattering cross section in a simplified model of dark matter production involving an axial-vector operator, Dirac DM and couplings $g_q = 0.25$ and $g_\chi = 1$ as a function of the dark matter mass m_χ . Also shown are results from three direct dark matter search experiments [72–74].

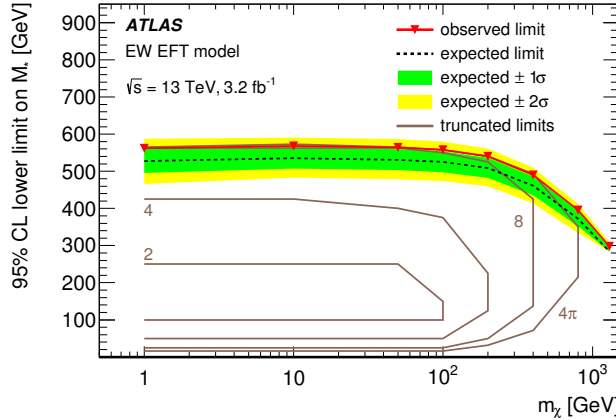


Figure 8: The observed and expected 95% CL limits on M_* for a dimension-7 operator EFT model with a contact interaction of type $\gamma\gamma\chi\chi$ as a function of dark matter mass m_χ . Results where EFT truncation is applied are also shown, assuming representative coupling values of 2, 4, 8 and 4π .

values of g^* is shown in Fig. 8: for the maximal coupling value of 4π , the truncation has almost no effect; for lower coupling values, the exclusion limits are confined to a smaller area of the parameter space, and no limit can be set for a coupling value of unity. For very low values of M_* , most events would fail the centre-of-mass energy truncation requirement, therefore, the truncated limits are not able to exclude very low M_* values. The search excludes model values of M_* up to 570 GeV and effects of truncation for various coupling values are shown in the figure.

In the ADD model of LED, the observed and expected 95% CL lower limits on the fundamental Planck mass M_D for various values of n are shown in Fig. 9. The values of M_D excluded at 95% CL are larger for larger n values: this is explained by the increase of the cross section at the centre-of-mass energy of 13 TeV with increasing n , which is an expected behaviour for values of M_D which are not large with respect to the centre-of-mass energy. Results incorporating truncation in the phase-space region where the model implementation is not valid are also shown. This consists in suppressing the graviton production cross section by a factor M_D^4/s^2 in events with centre-of-mass energy $\sqrt{s} > M_D$. The procedure is repeated iteratively with the new truncated limit until it converges, i.e., until the difference between the new truncated limit and the one obtained in the previous iteration differ by less than 0.1σ . It results in a decrease of the 95% CL limit on M_D . The search sets limits that are more stringent than those from LHC Run 1, excluding M_D up to about 2.3 TeV for $n = 2$ and up to 2.8 TeV for $n = 6$; the limit values are reduced by 20 to 40% depending on n when applying a truncation procedure.

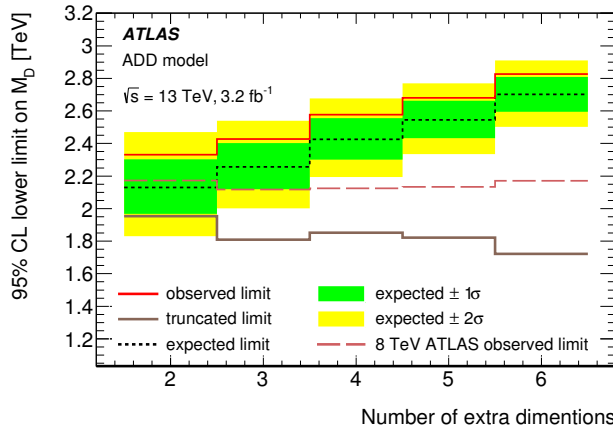


Figure 9: The observed and expected 95% CL lower limits on the mass scale M_D in the ADD models of large extra dimensions, for several values of the number of extra dimensions. The untruncated limits from the search of 8 TeV ATLAS data [7] are shown for comparison. The limit with truncation is also shown.

10 Conclusion

Results are reported on a search for new phenomena in events with a high- p_T photon and large missing transverse momentum in pp collisions at $\sqrt{s} = 13$ TeV at the LHC, using data collected by the ATLAS experiment corresponding to an integrated luminosity of 3.2 fb^{-1} . The observed data are consistent with the Standard Model expectations. The observed (expected) upper limits on the fiducial cross section for the production of events with a photon and large missing transverse momentum are 17.8 (25.5) fb at 95% CL and 14.6 (21.7) fb at 90% CL. For the simplified DM model considered, the search excludes mediator masses below 710 GeV for χ masses below 150 GeV. For the EW-EFT model values of M_* up to 570 GeV are excluded and the effect of truncation for various coupling values is reported. For the ADD model the search sets limits that are more stringent than in the Run 1 data search, excluding M_D up to about 2.3 TeV for $n = 2$ and up to 2.8 TeV for $n = 6$; the limit values are reduced by 20–40% depending on n when applying a truncation procedure.

Acknowledgements

We thank CERN for the very successful operation of the LHC, as well as the support staff from our institutions without whom ATLAS could not be operated efficiently.

We acknowledge the support of ANPCyT, Argentina; YerPhI, Armenia; ARC, Australia; BMWFW and FWF, Austria; ANAS, Azerbaijan; SSTC, Belarus; CNPq and FAPESP, Brazil; NSERC, NRC and CFI, Canada; CERN; CONICYT, Chile; CAS, MOST and NSFC, China; COLCIENCIAS, Colombia; MSMT CR, MPO CR and VSC CR, Czech Republic; DNRF and DNSRC, Denmark; IN2P3-CNRS, CEA-DSM/IRFU, France; GNSF, Georgia; BMBF, HGF, and MPG, Germany; GSRT, Greece; RGC, Hong Kong SAR, China; ISF, I-CORE and Benoziyo Center, Israel; INFN, Italy; MEXT and JSPS, Japan; CNRST, Morocco; FOM and NWO, Netherlands; RCN, Norway; MNiSW and NCN, Poland; FCT, Portugal; MNE/IFA, Romania; MES of Russia and NRC KI, Russian Federation; JINR; MESTD, Serbia; MSSR, Slovakia; ARRS and MIZŠ, Slovenia; DST/NRF, South Africa; MINECO, Spain; SRC and

Wallenberg Foundation, Sweden; SERI, SNSF and Cantons of Bern and Geneva, Switzerland; MOST, Taiwan; TAEK, Turkey; STFC, United Kingdom; DOE and NSF, United States of America. In addition, individual groups and members have received support from BCKDF, the Canada Council, CANARIE, CRC, Compute Canada, FQRNT, and the Ontario Innovation Trust, Canada; EPLANET, ERC, FP7, Horizon 2020 and Marie Skłodowska-Curie Actions, European Union; Investissements d’Avenir Labex and Idex, ANR, Région Auvergne and Fondation Partager le Savoir, France; DFG and AvH Foundation, Germany; Herakleitos, Thales and Aristeia programmes co-financed by EU-ESF and the Greek NSRF; BSF, GIF and Minerva, Israel; BRF, Norway; Generalitat de Catalunya, Generalitat Valenciana, Spain; the Royal Society and Leverhulme Trust, United Kingdom.

The crucial computing support from all WLCG partners is acknowledged gratefully, in particular from CERN and the ATLAS Tier-1 facilities at TRIUMF (Canada), NDGF (Denmark, Norway, Sweden), CC-IN2P3 (France), KIT/GridKA (Germany), INFN-CNAF (Italy), NL-T1 (Netherlands), PIC (Spain), ASGC (Taiwan), RAL (UK) and BNL (USA) and in the Tier-2 facilities worldwide.

References

- [1] CDF Collaboration, T. Aaltonen et al.,
Search for large extra dimensions in final states containing one photon or jet and large missing transverse energy produced in $p\bar{p}$ collisions at $\sqrt{s} = 1.96$ TeV,
Phys. Rev. Lett. **101** (2008) 181602, arXiv:[0807.3132 \[hep-ex\]](#).
- [2] D0 Collaboration, V.M. Abazov et al., *Search for large extra dimensions via single photon plus missing energy final states at $\sqrt{s} = 1.96$ TeV*, *Phys. Rev. Lett.* **101** (2008) 011601,
arXiv:[0803.2137 \[hep-ex\]](#).
- [3] OPAL Collaboration, G. Abbiendi et al.,
Photonic events with missing energy in e^+e^- collisions at $\sqrt{s} = 189$ GeV,
Eur. Phys. J. C **18** (2000) 253–272, arXiv:[hep-ex/0005002](#).
- [4] L3 Collaboration, P. Achard, et al.,
Single photon and multiphoton events with missing energy in e^+e^- collisions at LEP,
Phys. Lett. B **587** (2004) 16–32, arXiv:[hep-ex/0402002](#).
- [5] DELPHI Collaboration, J. Abdallah et al.,
Photon events with missing energy in e^+e^- collisions at $\sqrt{s} = 130$ GeV to 209 GeV,
Eur. Phys. J. C **38** (2005) 395–411, arXiv:[hep-ex/0406019](#).
- [6] ATLAS Collaboration,
Search for dark matter candidates and large extra dimensions in events with a photon and missing transverse momentum in pp collision data at $\sqrt{s} = 7$ TeV with the ATLAS detector,
Phys. Rev. Lett. **110** (2013) 011802, arXiv:[1209.4625 \[hep-ex\]](#).
- [7] ATLAS Collaboration, *Search for new phenomena in events with a photon and missing transverse momentum in pp collisions at $\sqrt{s} = 8$ TeV with the ATLAS detector,*
Phys. Rev. D **91** (2015) 012008, *Phys. Rev. D* **92** (2015) 059903, arXiv:[1411.1559 \[hep-ex\]](#).
- [8] CMS Collaboration, *Search for Dark Matter and Large Extra Dimensions in pp Collisions Yielding a Photon and Missing Transverse Energy*, *Phys. Rev. Lett.* **108** (2012) 261803,
arXiv:[1204.0821 \[hep-ex\]](#).

- [9] CMS Collaboration, *Search for new phenomena in monophoton final states in proton-proton collisions at $\sqrt{s} = 8$ TeV*, *Phys. Lett. B* **755** (2016) 102–124, arXiv:[1410.8812 \[hep-ex\]](#).
- [10] G. Bertone, D. Hooper and J. Silk, *Particle dark matter: Evidence, candidates and constraints*, *Phys. Rept.* **405** (2005) 279–390, arXiv:[hep-ph/0404175](#).
- [11] J. Goodman et al., *Constraints on Dark Matter from Colliders*, *Phys. Rev. D* **82** (2010) 116010, arXiv:[1008.1783 \[hep-ph\]](#).
- [12] J. Abdallah et al., *Simplified Models for Dark Matter Searches at the LHC*, *Phys. Dark Univ.* **9-10** (2015) 8.
- [13] O. Buchmueller et al., *Characterising dark matter searches at colliders and direct detection experiments: Vector mediators*, *JHEP* **01** (2015) 037.
- [14] D. Abercrombie et al., *Dark Matter Benchmark Models for Early LHC Run-2 Searches: Report of the ATLAS/CMS Dark Matter Forum*, (2015), arXiv:[1507.00966 \[hep-ex\]](#).
- [15] G. Busoni et al., *On the Validity of the Effective Field Theory for Dark Matter Searches at the LHC*, *Phys. Lett. B* **728** (2014) 412.
- [16] U. H. A. Crivellin and A. Hibbs, *LHC constraints on gauge boson couplings to dark matter*, *Phys. Rev. D* **91** (2015) 074028, arXiv:[1501.00907 \[hep-ph\]](#).
- [17] N. Arkani-Hamed, S. Dimopoulos and G. Dvali, *The Hierarchy problem and new dimensions at a millimeter*, *Phys. Lett. B* **429** (1998) 263–272, arXiv:[hep-ph/9803315](#).
- [18] ATLAS Collaboration, *The ATLAS Experiment at the CERN Large Hadron Collider*, *JINST* **3** (2008) S08003.
- [19] M. Capeans et al., *ATLAS Insertable B-Layer Technical Design Report*, CERN-LHCC-2010-013, ATLAS-TDR-19 (2010), <http://cds.cern.ch/record/1291633>.
- [20] ATLAS Collaboration, *2015 start-up trigger menu and initial performance assessment of the ATLAS trigger using Run-2 data*, ATL-DAQ-PUB-2016-001 (2016), <http://cds.cern.ch/record/2136007>.
- [21] NNPDF Collaboration, R. D. Ball et al., *Parton distributions for the LHC Run II*, *JHEP* **04** (2015) 040, arXiv:[1410.8849 \[hep-ph\]](#).
- [22] J. Alwall et al., *The automated computation of tree-level and next-to-leading order differential cross sections, and their matching to parton shower simulations*, *JHEP* **07** (2014) 079, arXiv:[1405.0301 \[hep-ph\]](#).
- [23] T. Sjöstrand, S. Mrenna and P. Z. Skands, *A Brief Introduction to PYTHIA 8.1*, *Comput. Phys. Commun.* **178** (2008) 852–867, arXiv:[0710.3820 \[hep-ph\]](#).
- [24] NNPDF Collaboration, R. D. Ball et al., *Parton distributions with LHC data*, *Nucl. Phys. B* **867** (2013) 244–289, arXiv:[1207.1303 \[hep-ph\]](#).
- [25] NNPDF Collaboration, R. D. Ball et al., *Parton distributions with QED corrections*, *Nucl. Phys. B* **877** (2013) 290, arXiv:[1308.0598 \[hep-ph\]](#).
- [26] ATLAS Collaboration, *ATLAS Run 1 Pythia8 tunes*, ATL-PHYS-PUB-2014-021 (2014), <http://cds.cern.ch/record/1966419>.

- [27] T. Gleisberg et al., *Event generation with SHERPA 1.1*, JHEP **02** (2009) 007, arXiv:[0811.4622 \[hep-ph\]](#).
- [28] S. Schumann and F. Krauss, *A Parton shower algorithm based on Catani-Seymour dipole factorisation*, JHEP **03** (2008) 038, arXiv:[0709.1027 \[hep-ph\]](#).
- [29] S. Höche et al., *QCD matrix elements and truncated showers*, JHEP **05** (2009) 053, arXiv:[0903.1219 \[hep-ph\]](#).
- [30] H.-L. Lai et al., *New parton distributions for collider physics*, Phys. Rev. D **82** (2010) 074024, arXiv:[1007.2241 \[hep-ph\]](#).
- [31] T. Gleisberg and S. Höche, *Comix, a new matrix element generator*, JHEP **12** (2008) 039, arXiv:[0808.3674 \[hep-ph\]](#).
- [32] F. Caccioli, P. Maierhofer and S. Pozzorini, *Scattering Amplitudes with Open Loops*, Phys. Rev. Lett. **108** (2012) 111601, arXiv:[1111.5206 \[hep-ph\]](#).
- [33] S. Höche et al., *QCD matrix elements + parton showers: The NLO case*, JHEP **04** (2013) 027, arXiv:[1207.5030 \[hep-ph\]](#).
- [34] ATLAS Collaboration, *Monte Carlo Generators for the Production of a W or Z/ γ^* Boson in Association with Jets at ATLAS in Run 2*, ATL-PHYS-PUB-2016-003 (2016), <http://cds.cern.ch/record/2120133>.
- [35] D. J. Lange, *The EvtGen particle decay simulation package*, Nucl. Instrum. Meth. A **462** (2001) 152.
- [36] S. Alioli et al., *A general framework for implementing NLO calculations in shower Monte Carlo programs: the POWHEG BOX*, JHEP **06** (2010) 043, arXiv:[1002.2581 \[hep-ph\]](#).
- [37] S. Alioli et al., *NLO single-top production matched with shower in POWHEG: s- and t-channel contributions*, JHEP **09** (2009) 111, [Erratum: JHEP02,011(2010)], arXiv:[0907.4076 \[hep-ph\]](#).
- [38] P. Artoisenet et al., *Automatic spin-entangled decays of heavy resonances in Monte Carlo simulations*, JHEP **03** (2013) 015, arXiv:[1212.3460 \[hep-ph\]](#).
- [39] T. Sjöstrand, S. Mrenna and P. Skands, *PYTHIA 6.4 physics and manual*, JHEP **05** (2006) 026, arXiv:[hep-ph/0603175](#).
- [40] J. Pumplin et al., *New generation of parton distributions with uncertainties from global QCD analysis*, JHEP **07** (2002) 012, arXiv:[hep-ph/0201195](#).
- [41] P. Z. Skands, *Tuning Monte Carlo Generators: The Perugia Tunes*, Phys. Rev. D **82** (2010) 074018, arXiv:[1005.3457 \[hep-ph\]](#).
- [42] ATLAS Collaboration, *Further ATLAS tunes of Pythia 6 and Pythia 8*, ATL-PHYS-PUB-2011-014 (2011), <http://cds.cern.ch/record/1400677>.
- [43] A. Martin et al., *Parton distributions for the LHC*, Eur. Phys. J. C **63** (2009) 189–285, arXiv:[0901.0002 \[hep-ph\]](#).
- [44] ATLAS Collaboration, *The ATLAS Simulation Infrastructure*, Eur. Phys. J. C **70** (2010) 823–874, arXiv:[1005.4568 \[physics.ins-det\]](#).

- [45] GEANT4 collaboration, Agostinelli, S. and others, *GEANT4: A Simulation toolkit*, *Nucl. Instrum. Methods Phys. Res., Sect. A* **506** (2003) 250–303.
- [46] ATLAS Collaboration, *Expected photon performance in the ATLAS experiment*, ATL-PHYS-PUB-2011-007 (2011), <http://cds.cern.ch/record/1345329>.
- [47] ATLAS Collaboration, *Electron and photon energy calibration with the ATLAS detector using LHC Run 1 data*, *Eur. Phys. J. C* **74** (2014) 3071, arXiv:[1407.5063 \[hep-ex\]](https://arxiv.org/abs/1407.5063).
- [48] ATLAS Collaboration, *Measurements of the photon identification efficiency with the ATLAS detector using 4.9 fb^{-1} of pp collision data collected in 2011*, ATLAS-CONF-2012-123, (2012), <http://cds.cern.ch/record/1473426>.
- [49] ATLAS Collaboration, *Muon reconstruction performance of the ATLAS detector in proton–proton collision data at 13 TeV*, *Eur. Phys. J. C* **76** (2016) 292, arXiv:[1603.05598 \[hep-ph\]](https://arxiv.org/abs/1603.05598).
- [50] M. Cacciari, G. P. Salam and G. Soyez, *The anti- k_t jet clustering algorithm*, *JHEP* **04** (2008) 063, arXiv:[0802.1189 \[hep-ph\]](https://arxiv.org/abs/0802.1189).
- [51] M. Cacciari and G. P. Salam, *Dispelling the N^3 myth for the k_t jet-finder*, *Phys. Lett. B* **641** (2006) 57–61, arXiv:[hep-ph/0512210](https://arxiv.org/abs/hep-ph/0512210).
- [52] ATLAS Collaboration, *Jet energy measurement with the ATLAS detector in proton-proton collisions at $\sqrt{s} = 7 \text{ TeV}$* , *Eur. Phys. J. C* **73** (2013) 2304, arXiv:[1112.6426 \[hep-ex\]](https://arxiv.org/abs/1112.6426).
- [53] ATLAS Collaboration, *Single hadron response measurement and calorimeter jet energy scale uncertainty with the ATLAS detector at the LHC*, *Eur. Phys. J. C* **73** (2013) 2305, arXiv:[1203.1302 \[hep-ex\]](https://arxiv.org/abs/1203.1302).
- [54] ATLAS Collaboration, *Tagging and suppression of pileup jets with the ATLAS detector*, ATLAS-CONF-2014-018, (2012), <http://cds.cern.ch/record/1700870>.
- [55] ATLAS Collaboration, *Performance of Missing Transverse Momentum Reconstruction in Proton-Proton Collisions at 7 TeV with ATLAS*, *Eur. Phys. J. C* **72** (2012) 1844, arXiv:[1108.5602 \[hep-ex\]](https://arxiv.org/abs/1108.5602).
- [56] ATLAS Collaboration, *Expected performance of missing transverse momentum reconstruction for the ATLAS detector at 13 TeV*, ATL-PHYS-PUB-2015-023 (2016), <http://cds.cern.ch/record/2013489>.
- [57] ATLAS Collaboration, *Measurement of the inclusive isolated prompt photon cross section in pp collisions at $\sqrt{s} = 7 \text{ TeV}$ with the ATLAS detector*, *Phys. Rev. D* **83** (2011) 052005, arXiv:[1012.4389 \[hep-ex\]](https://arxiv.org/abs/1012.4389).
- [58] ATLAS Collaboration, *Improved luminosity determination in pp collisions at $\sqrt{s} = 7 \text{ TeV}$ using the ATLAS detector at the LHC*, *Eur. Phys. J. C* **73** (2013) 2518, arXiv:[1302.4393 \[hep-ex\]](https://arxiv.org/abs/1302.4393).
- [59] ATLAS Collaboration, *Selection of jets produced in proton-proton collisions with the ATLAS detector using 2011 data*, ATLAS-CONF-2012-020, (2012), <http://cds.cern.ch/record/1430034>.
- [60] M. Baak et al., *HistFitter software framework for statistical data analysis*, *Eur. Phys. J. C* **75** (2015) 153, arXiv:[1410.1280 \[hep-ex\]](https://arxiv.org/abs/1410.1280).

- [61] ATLAS Collaboration, *Measurement of the inclusive isolated prompt photon cross section in pp collisions at 7 TeV with the ATLAS detector*, *Phys. Rev. D* **83** (2011) 052005, arXiv:[1012.04389 \[hep-ph\]](https://arxiv.org/abs/1012.04389).
- [62] M. Grazzini et al., *Wgamma and Zgamma production at the LHC in NNLO QCD*, (2016), arXiv:[1601.06751 \[hep-ph\]](https://arxiv.org/abs/1601.06751).
- [63] J. Butterworth et al., *PDF4LHC recommendations for LHC Run II*, (2015), arXiv:[1510.03865 \[hep-ph\]](https://arxiv.org/abs/1510.03865).
- [64] A. Buckley et al., *LHAPDF6: parton density access in the LHC precision era*, (2014), arXiv:[1412.7420 \[hep-ph\]](https://arxiv.org/abs/1412.7420).
- [65] ATLAS Collaboration, *Jet energy resolution and selection efficiency relative to track jets from in-situ techniques with the ATLAS Detector Using Proton-Proton Collisions at a Center of Mass Energy $\sqrt{s} = 7 \text{ TeV}$* , ATLAS-CONF-2010-054, (2010), <http://cds.cern.ch/record/1281311>.
- [66] A. L. Read, *Presentation of search results: The CL(s) technique*, *J. Phys. G* **28** (2002) 2693–2704.
- [67] T. Junk, *Confidence level computation for combining searches with small statistics*, *Nucl. Instrum. Methods Phys. Res., Sect. A* **434** (1999) 435–443, arXiv:[hep-ex/9902006](https://arxiv.org/abs/hep-ex/9902006).
- [68] G. Cowan et al., *Asymptotic formulae for likelihood-based tests of new physics*, *Eur. Phys. J. C* **71** (2011) 1554, arXiv:[1007.1727 \[physics.data-an\]](https://arxiv.org/abs/1007.1727).
- [69] F. Kahlhoefer et al., *Implications of unitarity and gauge invariance for simplified dark matter models*, *JHEP* (2016) 016, arXiv:[1510.02110 \[hep-ph\]](https://arxiv.org/abs/1510.02110).
- [70] WMAP Collaboration, G. Hinshaw et al., *Nine-year Wilkinson Microwave Anisotropy Probe (WMAP) Observations: Cosmological Parameter Results*, *Astrophys. J. Suppl.* **208** (2013), arXiv:[1212.5226 \[astro-ph.CO\]](https://arxiv.org/abs/1212.5226).
- [71] A. Boveia et al., *Recommendations on presenting LHC searches for missing transverse energy signals using simplified s-channel models of dark matter*, (2016), arXiv:[1603.04156 \[hep-ph\]](https://arxiv.org/abs/1603.04156).
- [72] PICO Collaboration, C. Amole et al., *Dark Matter Search Results from the PICO-2L C3F8 Bubble Chamber*, *Phys. Rev. Lett.* **114** (2015) 231302, arXiv:[1503.00008 \[astro-ph.CO\]](https://arxiv.org/abs/1503.00008).
- [73] XENON100 Collaboration, E. Aprile et al., *Limits on spin-dependent WIMP-nucleon cross sections from 225 live days of XENON100 data*, *Phys. Rev. Lett.* **111** (2013) 021301, arXiv:[1301.6620 \[astro-ph.CO\]](https://arxiv.org/abs/1301.6620).
- [74] LUX Collaboration, D. S. Akerib et al., *First spin-dependent WIMP-nucleon cross section limits from the LUX experiment*, (2016), arXiv:[1602.03489 \[hep-ex\]](https://arxiv.org/abs/1602.03489).
- [75] D. Racco et al., *Robust collider limits on heavy-mediator Dark Matter*, *J. High Energy Phys.* **05** (2015) 009, arXiv:[1502.04701 \[hep-ph\]](https://arxiv.org/abs/1502.04701).

The ATLAS Collaboration

M. Aaboud^{136d}, G. Aad⁸⁷, B. Abbott¹¹⁴, J. Abdallah⁶⁵, O. Abdinov¹², B. Abelsoos¹¹⁸, R. Aben¹⁰⁸, O.S. AbouZeid¹³⁸, N.L. Abraham¹⁵⁰, H. Abramowicz¹⁵⁴, H. Abreu¹⁵³, R. Abreu¹¹⁷, Y. Abulaiti^{147a,147b}, B.S. Acharya^{164a,164b,a}, L. Adamczyk^{40a}, D.L. Adams²⁷, J. Adelman¹⁰⁹, S. Adomeit¹⁰¹, T. Adye¹³², A.A. Affolder⁷⁶, T. Agatonovic-Jovin¹⁴, J. Agricola⁵⁶, J.A. Aguilar-Saavedra^{127a,127f}, S.P. Ahlen²⁴, F. Ahmadov^{67,b}, G. Aielli^{134a,134b}, H. Akerstedt^{147a,147b}, T.P.A. Åkesson⁸³, A.V. Akimov⁹⁷, G.L. Alberghi^{22a,22b}, J. Albert¹⁶⁹, S. Albrand⁵⁷, M.J. Alconada Verzini⁷³, M. Alekса³², I.N. Aleksandrov⁶⁷, C. Alexa^{28b}, G. Alexander¹⁵⁴, T. Alexopoulos¹⁰, M. Alhroob¹¹⁴, M. Aliev^{75a,75b}, G. Alimonti^{93a}, J. Alison³³, S.P. Alkire³⁷, B.M.M. Allbrooke¹⁵⁰, B.W. Allen¹¹⁷, P.P. Allport¹⁹, A. Aloisio^{105a,105b}, A. Alonso³⁸, F. Alonso⁷³, C. Alpigiani¹³⁹, M. Alstaty⁸⁷, B. Alvarez Gonzalez³², D. Álvarez Piqueras¹⁶⁷, M.G. Alviggi^{105a,105b}, B.T. Amadio¹⁶, K. Amako⁶⁸, Y. Amaral Coutinho^{26a}, C. Amelung²⁵, D. Amidei⁹¹, S.P. Amor Dos Santos^{127a,127c}, A. Amorim^{127a,127b}, S. Amoroso³², G. Amundsen²⁵, C. Anastopoulos¹⁴⁰, L.S. Ansu⁵¹, N. Andari¹⁰⁹, T. Andeen¹¹, C.F. Anders^{60b}, G. Anders³², J.K. Anders⁷⁶, K.J. Anderson³³, A. Andreazza^{93a,93b}, V. Andrei^{60a}, S. Angelidakis⁹, I. Angelozzi¹⁰⁸, P. Anger⁴⁶, A. Angerami³⁷, F. Anghinolfi³², A.V. Anisenkov^{110,c}, N. Anjos¹³, A. Annovi^{125a,125b}, M. Antonelli⁴⁹, A. Antonov⁹⁹, F. Anulli^{133a}, M. Aoki⁶⁸, L. Aperio Bella¹⁹, G. Arabidze⁹², Y. Arai⁶⁸, J.P. Araque^{127a}, A.T.H. Arce⁴⁷, F.A. Arduh⁷³, J.-F. Arguin⁹⁶, S. Argyropoulos⁶⁵, M. Arik^{20a}, A.J. Armbruster¹⁴⁴, L.J. Armitage⁷⁸, O. Arnaez³², H. Arnold⁵⁰, M. Arratia³⁰, O. Arslan²³, A. Artamonov⁹⁸, G. Artoni¹²¹, S. Artz⁸⁵, S. Asai¹⁵⁶, N. Asbah⁴⁴, A. Ashkenazi¹⁵⁴, B. Åsman^{147a,147b}, L. Asquith¹⁵⁰, K. Assamagan²⁷, R. Astalos^{145a}, M. Atkinson¹⁶⁶, N.B. Atlay¹⁴², K. Augsten¹²⁹, G. Avolio³², B. Axen¹⁶, M.K. Ayoub¹¹⁸, G. Azuelos^{96,d}, M.A. Baak³², A.E. Baas^{60a}, M.J. Baca¹⁹, H. Bachacou¹³⁷, K. Bachas^{75a,75b}, M. Backes³², M. Backhaus³², P. Bagiacchi^{133a,133b}, P. Bagnaia^{133a,133b}, Y. Bai^{35a}, J.T. Barnes¹³², O.K. Baker¹⁷⁶, E.M. Baldin^{110,c}, P. Balek¹³⁰, T. Balestri¹⁴⁹, F. Balli¹³⁷, W.K. Balunas¹²³, E. Banas⁴¹, Sw. Banerjee^{173,e}, A.A.E. Bannoura¹⁷⁵, L. Barak³², E.L. Barberio⁹⁰, D. Barberis^{52a,52b}, M. Barbero⁸⁷, T. Barillari¹⁰², M. Barisonzi^{164a,164b}, T. Barklow¹⁴⁴, N. Barlow³⁰, S.L. Barnes⁸⁶, B.M. Barnett¹³², R.M. Barnett¹⁶, Z. Barnovska⁵, A. Baroncelli^{135a}, G. Barone²⁵, A.J. Barr¹²¹, L. Barranco Navarro¹⁶⁷, F. Barreiro⁸⁴, J. Barreiro Guimarães da Costa^{35a}, R. Bartoldus¹⁴⁴, A.E. Barton⁷⁴, P. Bartos^{145a}, A. Basalaev¹²⁴, A. Bassalat¹¹⁸, R.L. Bates⁵⁵, S.J. Batista¹⁵⁹, J.R. Batley³⁰, M. Battaglia¹³⁸, M. Bauce^{133a,133b}, F. Bauer¹³⁷, H.S. Bawa^{144,f}, J.B. Beacham¹¹², M.D. Beattie⁷⁴, T. Beau⁸², P.H. Beauchemin¹⁶², P. Bechtle²³, H.P. Beck^{18,g}, K. Becker¹²¹, M. Becker⁸⁵, M. Beckingham¹⁷⁰, C. Becot¹¹¹, A.J. Beddall^{20e}, A. Beddall^{20b}, V.A. Bednyakov⁶⁷, M. Bedognetti¹⁰⁸, C.P. Bee¹⁴⁹, L.J. Beemster¹⁰⁸, T.A. Beermann³², M. Begel²⁷, J.K. Behr⁴⁴, C. Belanger-Champagne⁸⁹, A.S. Bell⁸⁰, G. Bella¹⁵⁴, L. Bellagamba^{22a}, A. Bellerive³¹, M. Bellomo⁸⁸, K. Belotskiy⁹⁹, O. Beltramello³², N.L. Belyaev⁹⁹, O. Benary¹⁵⁴, D. Benchekroun^{136a}, M. Bender¹⁰¹, K. Bendtz^{147a,147b}, N. Benekos¹⁰, Y. Benhammou¹⁵⁴, E. Benhar Noccioli¹⁷⁶, J. Benitez⁶⁵, D.P. Benjamin⁴⁷, J.R. Bensinger²⁵, S. Bentvelsen¹⁰⁸, L. Beresford¹²¹, M. Beretta⁴⁹, D. Berge¹⁰⁸, E. Bergeaas Kuutmann¹⁶⁵, N. Berger⁵, J. Beringer¹⁶, S. Berlendis⁵⁷, N.R. Bernard⁸⁸, C. Bernius¹¹¹, F.U. Bernlochner²³, T. Berry⁷⁹, P. Berta¹³⁰, C. Bertella⁸⁵, G. Bertoli^{147a,147b}, F. Bertolucci^{125a,125b}, I.A. Bertram⁷⁴, C. Bertsche⁴⁴, D. Bertsche¹¹⁴, G.J. Besjes³⁸, O. Bessidskaia Bylund^{147a,147b}, M. Bessner⁴⁴, N. Besson¹³⁷, C. Betancourt⁵⁰, S. Bethke¹⁰², A.J. Bevan⁷⁸, W. Bhimji¹⁶, R.M. Bianchi¹²⁶, L. Bianchini²⁵, M. Bianco³², O. Biebel¹⁰¹, D. Biedermann¹⁷, R. Bielski⁸⁶, N.V. Biesuz^{125a,125b}, M. Biglietti^{135a}, J. Bilbao De Mendizabal⁵¹, H. Bilonok⁴⁹, M. Bindi⁵⁶, S. Binet¹¹⁸, A. Bingul^{20b}, C. Bini^{133a,133b}, S. Biondi^{22a,22b}, D.M. Bjergaard⁴⁷, C.W. Black¹⁵¹, J.E. Black¹⁴⁴, K.M. Black²⁴, D. Blackburn¹³⁹, R.E. Blair⁶, J.-B. Blanchard¹³⁷, J.E. Blanco⁷⁹, T. Blazek^{145a}, I. Bloch⁴⁴, C. Blocker²⁵, W. Blum^{85,*}, U. Blumenschein⁵⁶, S. Blunier^{34a},

G.J. Bobbink¹⁰⁸, V.S. Bobrovnikov^{110,c}, S.S. Bocchetta⁸³, A. Bocci⁴⁷, C. Bock¹⁰¹, M. Boehler⁵⁰,
 D. Boerner¹⁷⁵, J.A. Bogaerts³², D. Bogavac¹⁴, A.G. Bogdanchikov¹¹⁰, C. Bohm^{147a}, V. Boisvert⁷⁹,
 P. Bokan¹⁴, T. Bold^{40a}, A.S. Boldyrev^{164a,164c}, M. Bomben⁸², M. Bona⁷⁸, M. Boonekamp¹³⁷,
 A. Borisov¹³¹, G. Borissov⁷⁴, J. Bortfeldt¹⁰¹, D. Bortoletto¹²¹, V. Bortolotto^{62a,62b,62c}, K. Bos¹⁰⁸,
 D. Boscherini^{22a}, M. Bosman¹³, J.D. Bossio Sola²⁹, J. Boudreau¹²⁶, J. Bouffard²,
 E.V. Bouhova-Thacker⁷⁴, D. Boumediene³⁶, C. Bourdarios¹¹⁸, S.K. Boutle⁵⁵, A. Boveia³², J. Boyd³²,
 I.R. Boyko⁶⁷, J. Bracinik¹⁹, A. Brandt⁸, G. Brandt⁵⁶, O. Brandt^{60a}, U. Bratzler¹⁵⁷, B. Brau⁸⁸,
 J.E. Brau¹¹⁷, H.M. Braun^{175,*}, W.D. Breaden Madden⁵⁵, K. Brendlinger¹²³, A.J. Brennan⁹⁰,
 L. Brenner¹⁰⁸, R. Brenner¹⁶⁵, S. Bressler¹⁷², T.M. Bristow⁴⁸, D. Britton⁵⁵, D. Britzger⁴⁴, F.M. Brochu³⁰,
 I. Brock²³, R. Brock⁹², G. Brooijmans³⁷, T. Brooks⁷⁹, W.K. Brooks^{34b}, J. Brosamer¹⁶, E. Brost¹¹⁷,
 J.H. Broughton¹⁹, P.A. Bruckman de Renstrom⁴¹, D. Bruncko^{145b}, R. Bruneliere⁵⁰, A. Bruni^{22a},
 G. Bruni^{22a}, L.S. Bruni¹⁰⁸, BH Brunt³⁰, M. Bruschi^{22a}, N. Bruscino²³, P. Bryant³³, L. Bryngemark⁸³,
 T. Buanes¹⁵, Q. Buat¹⁴³, P. Buchholz¹⁴², A.G. Buckley⁵⁵, I.A. Budagov⁶⁷, F. Buehrer⁵⁰, M.K. Bugge¹²⁰,
 O. Bulekov⁹⁹, D. Bullock⁸, H. Burckhart³², S. Burdin⁷⁶, C.D. Burgard⁵⁰, B. Burghgrave¹⁰⁹, K. Burka⁴¹,
 S. Burke¹³², I. Burmeister⁴⁵, E. Busato³⁶, D. Büscher⁵⁰, V. Büscher⁸⁵, P. Bussey⁵⁵, J.M. Butler²⁴,
 C.M. Buttar⁵⁵, J.M. Butterworth⁸⁰, P. Butti¹⁰⁸, W. Buttlinger²⁷, A. Buzatu⁵⁵, A.R. Buzykaev^{110,c},
 S. Cabrera Urbán¹⁶⁷, D. Caforio¹²⁹, V.M. Cairo^{39a,39b}, O. Cakir^{4a}, N. Calace⁵¹, P. Calafuria¹⁶,
 A. Calandri⁸⁷, G. Calderini⁸², P. Calfayan¹⁰¹, L.P. Caloba^{26a}, D. Calvet³⁶, S. Calvet³⁶, T.P. Calvet⁸⁷,
 R. Camacho Toro³³, S. Camarda³², P. Camarri^{134a,134b}, D. Cameron¹²⁰, R. Caminal Armadans¹⁶⁶,
 C. Camincher⁵⁷, S. Campana³², M. Campanelli⁸⁰, A. Camplani^{93a,93b}, A. Campoverde¹⁴⁹,
 V. Canale^{105a,105b}, A. Canepa^{160a}, M. Cano Bret^{35e}, J. Cantero¹¹⁵, R. Cantrill^{127a}, T. Cao⁴²,
 M.D.M. Capeans Garrido³², I. Caprini^{28b}, M. Caprini^{28b}, M. Capua^{39a,39b}, R. Caputo⁸⁵, R.M. Carbone³⁷,
 R. Cardarelli^{134a}, F. Cardillo⁵⁰, T. Carli³², G. Carlino^{105a}, L. Carminati^{93a,93b}, S. Caron¹⁰⁷,
 E. Carquin^{34b}, G.D. Carrillo-Montoya³², J.R. Carter³⁰, J. Carvalho^{127a,127c}, D. Casadei¹⁹,
 M.P. Casado^{13,h}, M. Casolino¹³, D.W. Casper¹⁶³, E. Castaneda-Miranda^{146a}, R. Castelijn¹⁰⁸,
 A. Castelli¹⁰⁸, V. Castillo Gimenez¹⁶⁷, N.F. Castro^{127a,i}, A. Catinaccio³², J.R. Catmore¹²⁰, A. Cattai³²,
 J. Caudron⁸⁵, V. Cavalieri¹⁶⁶, E. Cavallaro¹³, D. Cavalli^{93a}, M. Cavalli-Sforza¹³, V. Cavasinni^{125a,125b},
 F. Ceradini^{135a,135b}, L. Cerdá Alberich¹⁶⁷, B.C. Cerio⁴⁷, A.S. Cerqueira^{26b}, A. Cerri¹⁵⁰, L. Cerrito⁷⁸,
 F. Cerutti¹⁶, M. Cerv³², A. Cervelli¹⁸, S.A. Cetin^{20d}, A. Chafaq^{136a}, D. Chakraborty¹⁰⁹,
 I. Chalupkova¹³⁰, S.K. Chan⁵⁹, Y.L. Chan^{62a}, P. Chang¹⁶⁶, J.D. Chapman³⁰, D.G. Charlton¹⁹,
 A. Chatterjee⁵¹, C.C. Chau¹⁵⁹, C.A. Chavez Barajas¹⁵⁰, S. Che¹¹², S. Cheatham⁷⁴, A. Chegwidden⁹²,
 S. Chekanov⁶, S.V. Chekulaev^{160a}, G.A. Chelkov^{67,j}, M.A. Chelstowska⁹¹, C. Chen⁶⁶, H. Chen²⁷,
 K. Chen¹⁴⁹, S. Chen^{35c}, S. Chen¹⁵⁶, X. Chen^{35f}, Y. Chen⁶⁹, H.C. Cheng⁹¹, H.J. Cheng^{35a}, Y. Cheng³³,
 A. Cheplakov⁶⁷, E. Cheremushkina¹³¹, R. Cherkaoui El Moursli^{136e}, V. Chernyatin^{27,*}, E. Cheu⁷,
 L. Chevalier¹³⁷, V. Chiarella⁴⁹, G. Chiarelli^{125a,125b}, G. Chiodini^{75a}, A.S. Chisholm¹⁹, A. Chitan^{28b},
 M.V. Chizhov⁶⁷, K. Choi⁶³, A.R. Chomont³⁶, S. Chouridou⁹, B.K.B. Chow¹⁰¹, V. Christodoulou⁸⁰,
 D. Chromek-Burckhart³², J. Chudoba¹²⁸, A.J. Chuinard⁸⁹, J.J. Chwastowski⁴¹, L. Chytka¹¹⁶,
 G. Ciapetti^{133a,133b}, A.K. Ciftci^{4a}, D. Cinca⁵⁵, V. Cindro⁷⁷, I.A. Cioara²³, A. Ciocio¹⁶, F. Cirotto^{105a,105b},
 Z.H. Citron¹⁷², M. Citterio^{93a}, M. Ciubancan^{28b}, A. Clark⁵¹, B.L. Clark⁵⁹, M.R. Clark³⁷, P.J. Clark⁴⁸,
 R.N. Clarke¹⁶, C. Clement^{147a,147b}, Y. Coadou⁸⁷, M. Cobal^{164a,164c}, A. Coccaro⁵¹, J. Cochran⁶⁶,
 L. Coffey²⁵, L. Colasurdo¹⁰⁷, B. Cole³⁷, A.P. Colijn¹⁰⁸, J. Collot⁵⁷, T. Colombo³², G. Compostella¹⁰²,
 P. Conde Muiño^{127a,127b}, E. Coniavitis⁵⁰, S.H. Connell^{146b}, I.A. Connolly⁷⁹, V. Consorti⁵⁰,
 S. Constantinescu^{28b}, G. Conti³², F. Conventi^{105a,k}, M. Cooke¹⁶, B.D. Cooper⁸⁰, A.M. Cooper-Sarkar¹²¹,
 K.J.R. Cormier¹⁵⁹, T. Cornelissen¹⁷⁵, M. Corradi^{133a,133b}, F. Corriveau^{89,l}, A. Corso-Radu¹⁶³,
 A. Cortes-Gonzalez¹³, G. Cortiana¹⁰², G. Costa^{93a}, M.J. Costa¹⁶⁷, D. Costanzo¹⁴⁰, G. Cottin³⁰,
 G. Cowan⁷⁹, B.E. Cox⁸⁶, K. Cranmer¹¹¹, S.J. Crawley⁵⁵, G. Cree³¹, S. Crépé-Renaudin⁵⁷, F. Crescioli⁸²,
 W.A. Cribbs^{147a,147b}, M. Crispin Ortuzar¹²¹, M. Cristinziani²³, V. Croft¹⁰⁷, G. Crosetti^{39a,39b},

T. Cuhadar Donszelmann¹⁴⁰, J. Cummings¹⁷⁶, M. Curatolo⁴⁹, J. Cúth⁸⁵, C. Cuthbert¹⁵¹, H. Czirr¹⁴²,
 P. Czodrowski³, G. D'amen^{22a,22b}, S. D'Auria⁵⁵, M. D'Onofrio⁷⁶,
 M.J. Da Cunha Sargedas De Sousa^{127a,127b}, C. Da Via⁸⁶, W. Dabrowski^{40a}, T. Dado^{145a}, T. Dai⁹¹,
 O. Dale¹⁵, F. Dallaire⁹⁶, C. Dallapiccola⁸⁸, M. Dam³⁸, J.R. Dandoy³³, N.P. Dang⁵⁰, A.C. Daniells¹⁹,
 N.S. Dann⁸⁶, M. Danninger¹⁶⁸, M. Dano Hoffmann¹³⁷, V. Dao⁵⁰, G. Darbo^{52a}, S. Darmora⁸,
 J. Dassoulas³, A. Dattagupta⁶³, W. Davey²³, C. David¹⁶⁹, T. Davidek¹³⁰, M. Davies¹⁵⁴, P. Davison⁸⁰,
 E. Dawe⁹⁰, I. Dawson¹⁴⁰, R.K. Daya-Ishmukhametova⁸⁸, K. De⁸, R. de Asmundis^{105a},
 A. De Benedetti¹¹⁴, S. De Castro^{22a,22b}, S. De Cecco⁸², N. De Groot¹⁰⁷, P. de Jong¹⁰⁸, H. De la Torre⁸⁴,
 F. De Lorenzi⁶⁶, A. De Maria⁵⁶, D. De Pedis^{133a}, A. De Salvo^{133a}, U. De Sanctis¹⁵⁰, A. De Santo¹⁵⁰,
 J.B. De Vivie De Regie¹¹⁸, W.J. Dearnaley⁷⁴, R. Debbe²⁷, C. Debenedetti¹³⁸, D.V. Dedovich⁶⁷,
 N. Dehghanian³, I. Deigaard¹⁰⁸, M. Del Gaudio^{39a,39b}, J. Del Peso⁸⁴, T. Del Prete^{125a,125b},
 D. Delgove¹¹⁸, F. Deliot¹³⁷, C.M. Delitzsch⁵¹, M. Deliyergiyev⁷⁷, A. Dell'Acqua³², L. Dell'Asta²⁴,
 M. Dell'Orso^{125a,125b}, M. Della Pietra^{105a,k}, D. della Volpe⁵¹, M. Delmastro⁵, P.A. Delsart⁵⁷,
 C. Deluca¹⁰⁸, D.A. DeMarco¹⁵⁹, S. Demers¹⁷⁶, M. Demichev⁶⁷, A. Demilly⁸², S.P. Denisov¹³¹,
 D. Denysiuk¹³⁷, D. Derendarz⁴¹, J.E. Derkaoui^{136d}, F. Derue⁸², P. Dervan⁷⁶, K. Desch²³, C. Deterre⁴⁴,
 K. Dette⁴⁵, P.O. Deviveiros³², A. Dewhurst¹³², S. Dhaliwal²⁵, A. Di Ciacio^{134a,134b}, L. Di Ciacio⁵,
 W.K. Di Clemente¹²³, C. Di Donato^{133a,133b}, A. Di Girolamo³², B. Di Girolamo³², B. Di Micco^{135a,135b},
 R. Di Nardo³², A. Di Simone⁵⁰, R. Di Sipio¹⁵⁹, D. Di Valentino³¹, C. Diaconu⁸⁷, M. Diamond¹⁵⁹,
 F.A. Dias⁴⁸, M.A. Diaz^{34a}, E.B. Diehl⁹¹, J. Dietrich¹⁷, S. Diglio⁸⁷, A. Dimitrieva¹⁴, J. Dingfelder²³,
 P. Dita^{28b}, S. Dita^{28b}, F. Dittus³², F. Djama⁸⁷, T. Djobava^{53b}, J.I. Djuvsland^{60a}, M.A.B. do Vale^{26c},
 D. Dobos³², M. Dobre^{28b}, C. Doglioni⁸³, T. Dohmae¹⁵⁶, J. Dolejsi¹³⁰, Z. Dolezal¹³⁰,
 B.A. Dolgoshein^{99,*}, M. Donadelli^{26d}, S. Donati^{125a,125b}, P. Dondero^{122a,122b}, J. Donini³⁶, J. Dopke¹³²,
 A. Doria^{105a}, M.T. Dova⁷³, A.T. Doyle⁵⁵, E. Drechsler⁵⁶, M. Dris¹⁰, Y. Du^{35d}, J. Duarte-Campderros¹⁵⁴,
 E. Duchovni¹⁷², G. Duckeck¹⁰¹, O.A. Ducu^{96,m}, D. Duda¹⁰⁸, A. Dudarev³², E.M. Duffield¹⁶,
 L. Duflot¹¹⁸, L. Duguid⁷⁹, M. Dührssen³², M. Dumancic¹⁷², M. Dunford^{60a}, H. Duran Yildiz^{4a},
 M. Düren⁵⁴, A. Durglishvili^{53b}, D. Duschinger⁴⁶, B. Dutta⁴⁴, M. Dyndal^{40a}, C. Eckardt⁴⁴,
 K.M. Ecker¹⁰², R.C. Edgar⁹¹, N.C. Edwards⁴⁸, T. Eifert³², G. Eigen¹⁵, K. Einsweiler¹⁶, T. Ekelof¹⁶⁵,
 M. El Kacimi^{136c}, V. Ellajosyula⁸⁷, M. Ellert¹⁶⁵, S. Elles⁵, F. Ellinghaus¹⁷⁵, A.A. Elliot¹⁶⁹, N. Ellis³²,
 J. Elmsheuser²⁷, M. Elsing³², D. Emelyanov¹³², Y. Enari¹⁵⁶, O.C. Endner⁸⁵, M. Endo¹¹⁹, J.S. Ennis¹⁷⁰,
 J. Erdmann⁴⁵, A. Ereditato¹⁸, G. Ernis¹⁷⁵, J. Ernst², M. Ernst²⁷, S. Errede¹⁶⁶, E. Ertel⁸⁵, M. Escalier¹¹⁸,
 H. Esch⁴⁵, C. Escobar¹²⁶, B. Esposito⁴⁹, A.I. Etienne¹³⁷, E. Etzion¹⁵⁴, H. Evans⁶³, A. Ezhilov¹²⁴,
 F. Fabbri^{22a,22b}, L. Fabbri^{22a,22b}, G. Facini³³, R.M. Fakhrutdinov¹³¹, S. Falciano^{133a}, R.J. Falla⁸⁰,
 J. Faltova¹³⁰, Y. Fang^{35a}, M. Fanti^{93a,93b}, A. Farbin⁸, A. Farilla^{135a}, C. Farina¹²⁶, T. Farooque¹³,
 S. Farrell¹⁶, S.M. Farrington¹⁷⁰, P. Farthouat³², F. Fassi^{136e}, P. Fassnacht³², D. Fassouliotis⁹,
 M. Faucci Giannelli⁷⁹, A. Favaretto^{52a,52b}, W.J. Fawcett¹²¹, L. Fayard¹¹⁸, O.L. Fedin^{124,n}, W. Fedorko¹⁶⁸,
 S. Feigl¹²⁰, L. Feligioni⁸⁷, C. Feng^{35d}, E.J. Feng³², H. Feng⁹¹, A.B. Fenyuk¹³¹, L. Feremenga⁸,
 P. Fernandez Martinez¹⁶⁷, S. Fernandez Perez¹³, J. Ferrando⁵⁵, A. Ferrari¹⁶⁵, P. Ferrari¹⁰⁸, R. Ferrari^{122a},
 D.E. Ferreira de Lima^{60b}, A. Ferrer¹⁶⁷, D. Ferrere⁵¹, C. Ferretti⁹¹, A. Ferretto Parodi^{52a,52b}, F. Fiedler⁸⁵,
 A. Filipčič⁷⁷, M. Filipuzzi⁴⁴, F. Filthaut¹⁰⁷, M. Fincke-Keeler¹⁶⁹, K.D. Finelli¹⁵¹,
 M.C.N. Fiolhais^{127a,127c}, L. Fiorini¹⁶⁷, A. Firan⁴², A. Fischer², C. Fischer¹³, J. Fischer¹⁷⁵, W.C. Fisher⁹²,
 N. Flaschel⁴⁴, I. Fleck¹⁴², P. Fleischmann⁹¹, G.T. Fletcher¹⁴⁰, R.R.M. Fletcher¹²³, T. Flick¹⁷⁵,
 A. Floderus⁸³, L.R. Flores Castillo^{62a}, M.J. Flowerdew¹⁰², G.T. Forcolin⁸⁶, A. Formica¹³⁷, A. Forti⁸⁶,
 A.G. Foster¹⁹, D. Fournier¹¹⁸, H. Fox⁷⁴, S. Fracchia¹³, P. Francavilla⁸², M. Franchini^{22a,22b},
 D. Francis³², L. Franconi¹²⁰, M. Franklin⁵⁹, M. Frate¹⁶³, M. Fraternali^{122a,122b}, D. Freeborn⁸⁰,
 S.M. Fressard-Batraneanu³², F. Friedrich⁴⁶, D. Froidevaux³², J.A. Frost¹²¹, C. Fukunaga¹⁵⁷,
 E. Fullana Torregrossa⁸⁵, T. Fusayasu¹⁰³, J. Fuster¹⁶⁷, C. Gabaldon⁵⁷, O. Gabizon¹⁷⁵, A. Gabrielli^{22a,22b},
 A. Gabrielli¹⁶, G.P. Gach^{40a}, S. Gadatsch³², S. Gadomski⁵¹, G. Gagliardi^{52a,52b}, L.G. Gagnon⁹⁶,

P. Gagnon⁶³, C. Galea¹⁰⁷, B. Galhardo^{127a,127c}, E.J. Gallas¹²¹, B.J. Gallop¹³², P. Gallus¹²⁹, G. Galster³⁸, K.K. Gan¹¹², J. Gao^{35b,87}, Y. Gao⁴⁸, Y.S. Gao^{144,f}, F.M. Garay Walls⁴⁸, C. García¹⁶⁷, J.E. García Navarro¹⁶⁷, M. Garcia-Sciveres¹⁶, R.W. Gardner³³, N. Garelli¹⁴⁴, V. Garonne¹²⁰, A. Gascon Bravo⁴⁴, C. Gatti⁴⁹, A. Gaudiello^{52a,52b}, G. Gaudio^{122a}, B. Gaur¹⁴², L. Gauthier⁹⁶, I.L. Gavrilenko⁹⁷, C. Gay¹⁶⁸, G. Gaycken²³, E.N. Gazis¹⁰, Z. Gecse¹⁶⁸, C.N.P. Gee¹³², Ch. Geich-Gimbel²³, M. Geisen⁸⁵, M.P. Geisler^{60a}, C. Gemme^{52a}, M.H. Genest⁵⁷, C. Geng^{35b,o}, S. Gentile^{133a,133b}, S. George⁷⁹, D. Gerbaudo¹³, A. Gershon¹⁵⁴, S. Ghasemi¹⁴², H. Ghazlane^{136b}, M. Ghneimat²³, B. Giacobbe^{22a}, S. Giagu^{133a,133b}, P. Giannetti^{125a,125b}, B. Gibbard²⁷, S.M. Gibson⁷⁹, M. Gignac¹⁶⁸, M. Gilchriese¹⁶, T.P.S. Gillam³⁰, D. Gillberg³¹, G. Gilles¹⁷⁵, D.M. Gingrich^{3,d}, N. Giokaris⁹, M.P. Giordani^{164a,164c}, F.M. Giorgi^{22a}, F.M. Giorgi¹⁷, P.F. Giraud¹³⁷, P. Giromini⁵⁹, D. Giugni^{93a}, F. Giuli¹²¹, C. Giuliani¹⁰², M. Giulini^{60b}, B.K. Gjelsten¹²⁰, S. Gkaitatzis¹⁵⁵, I. Gkialas¹⁵⁵, E.L. Gkougkousis¹¹⁸, L.K. Gladilin¹⁰⁰, C. Glasman⁸⁴, J. Glatzer³², P.C.F. Glaysher⁴⁸, A. Glazov⁴⁴, M. Goblirsch-Kolb¹⁰², J. Godlewski⁴¹, S. Goldfarb⁹¹, T. Golling⁵¹, D. Golubkov¹³¹, A. Gomes^{127a,127b,127d}, R. Gonçalo^{127a}, J. Goncalves Pinto Firmino Da Costa¹³⁷, L. Gonella¹⁹, A. Gongadze⁶⁷, S. González de la Hoz¹⁶⁷, G. Gonzalez Parra¹³, S. Gonzalez-Sevilla⁵¹, L. Goossens³², P.A. Gorbounov⁹⁸, H.A. Gordon²⁷, I. Gorelov¹⁰⁶, B. Gorini³², E. Gorini^{75a,75b}, A. Gorišek⁷⁷, E. Gornicki⁴¹, A.T. Goshaw⁴⁷, C. Gössling⁴⁵, M.I. Gostkin⁶⁷, C.R. Goudet¹¹⁸, D. Goujdami^{136c}, A.G. Goussiou¹³⁹, N. Govender^{146b}, E. Gozani¹⁵³, L. Graber⁵⁶, I. Grabowska-Bold^{40a}, P.O.J. Gradin⁵⁷, P. Grafström^{22a,22b}, J. Gramling⁵¹, E. Gramstad¹²⁰, S. Grancagnolo¹⁷, V. Gratchev¹²⁴, P.M. Gravila^{28e}, H.M. Gray³², E. Graziani^{135a}, Z.D. Greenwood^{81,p}, C. Grefe²³, K. Gregersen⁸⁰, I.M. Gregor⁴⁴, P. Grenier¹⁴⁴, K. Grevtsov⁵, J. Griffiths⁸, A.A. Grillo¹³⁸, K. Grimm⁷⁴, S. Grinstein^{13,q}, Ph. Gris³⁶, J.-F. Grivaz¹¹⁸, S. Groh⁸⁵, J.P. Grohs⁴⁶, E. Gross¹⁷², J. Grosse-Knetter⁵⁶, G.C. Grossi⁸¹, Z.J. Grout¹⁵⁰, L. Guan⁹¹, W. Guan¹⁷³, J. Guenther¹²⁹, F. Guescini⁵¹, D. Guest¹⁶³, O. Gueta¹⁵⁴, E. Guido^{52a,52b}, T. Guillemin⁵, S. Guindon², U. Gul⁵⁵, C. Gumpert³², J. Guo^{35e}, Y. Guo^{35b,o}, S. Gupta¹²¹, G. Gustavino^{133a,133b}, P. Gutierrez¹¹⁴, N.G. Gutierrez Ortiz⁸⁰, C. Gutschow⁴⁶, C. Guyot¹³⁷, C. Gwenlan¹²¹, C.B. Gwilliam⁷⁶, A. Haas¹¹¹, C. Haber¹⁶, H.K. Hadavand⁸, N. Haddad^{136e}, A. Hadef⁸⁷, P. Haefner²³, S. Hageböck²³, Z. Hajduk⁴¹, H. Hakobyan^{177,*}, M. Haleem⁴⁴, J. Haley¹¹⁵, G. Halladjian⁹², G.D. Hallewell⁸⁷, K. Hamacher¹⁷⁵, P. Hamal¹¹⁶, K. Hamano¹⁶⁹, A. Hamilton^{146a}, G.N. Hamity¹⁴⁰, P.G. Hamnett⁴⁴, L. Han^{35b}, K. Hanagaki^{68,r}, K. Hanawa¹⁵⁶, M. Hance¹³⁸, B. Haney¹²³, P. Hanke^{60a}, R. Hanna¹³⁷, J.B. Hansen³⁸, J.D. Hansen³⁸, M.C. Hansen²³, P.H. Hansen³⁸, K. Hara¹⁶¹, A.S. Hard¹⁷³, T. Harenberg¹⁷⁵, F. Hariri¹¹⁸, S. Harkusha⁹⁴, R.D. Harrington⁴⁸, P.F. Harrison¹⁷⁰, F. Hartjes¹⁰⁸, N.M. Hartmann¹⁰¹, M. Hasegawa⁶⁹, Y. Hasegawa¹⁴¹, A. Hasib¹¹⁴, S. Hassani¹³⁷, S. Haug¹⁸, R. Hauser⁹², L. Hauswald⁴⁶, M. Havranek¹²⁸, C.M. Hawkes¹⁹, R.J. Hawkings³², D. Hayden⁹², C.P. Hays¹²¹, J.M. Hays⁷⁸, H.S. Hayward⁷⁶, S.J. Haywood¹³², S.J. Head¹⁹, T. Heck⁸⁵, V. Hedberg⁸³, L. Heelan⁸, S. Heim¹²³, T. Heim¹⁶, B. Heinemann¹⁶, J.J. Heinrich¹⁰¹, L. Heinrich¹¹¹, C. Heinz⁵⁴, J. Hejbal¹²⁸, L. Helary²⁴, S. Hellman^{147a,147b}, C. Helsens³², J. Henderson¹²¹, R.C.W. Henderson⁷⁴, Y. Heng¹⁷³, S. Henkelmann¹⁶⁸, A.M. Henriques Correia³², S. Henrot-Versille¹¹⁸, G.H. Herbert¹⁷, Y. Hernández Jiménez¹⁶⁷, G. Herten⁵⁰, R. Hertenberger¹⁰¹, L. Hervas³², G.G. Hesketh⁸⁰, N.P. Hessey¹⁰⁸, J.W. Hetherly⁴², R. Hickling⁷⁸, E. Higón-Rodriguez¹⁶⁷, E. Hill¹⁶⁹, J.C. Hill³⁰, K.H. Hiller⁴⁴, S.J. Hillier¹⁹, I. Hinchliffe¹⁶, E. Hines¹²³, R.R. Hinman¹⁶, M. Hirose¹⁵⁸, D. Hirschbuehl¹⁷⁵, J. Hobbs¹⁴⁹, N. Hod^{160a}, M.C. Hodgkinson¹⁴⁰, P. Hodgson¹⁴⁰, A. Hoecker³², M.R. Hoeferkamp¹⁰⁶, F. Hoenig¹⁰¹, D. Hohn²³, T.R. Holmes¹⁶, M. Homann⁴⁵, T.M. Hong¹²⁶, B.H. Hooberman¹⁶⁶, W.H. Hopkins¹¹⁷, Y. Horii¹⁰⁴, A.J. Horton¹⁴³, J.-Y. Hostachy⁵⁷, S. Hou¹⁵², A. Hoummada^{136a}, J. Howarth⁴⁴, M. Hrabovsky¹¹⁶, I. Hristova¹⁷, J. Hrvnac¹¹⁸, T. Hryna'ova⁵, A. Hrynevich⁹⁵, C. Hsu^{146c}, P.J. Hsu^{152,s}, S.-C. Hsu¹³⁹, D. Hu³⁷, Q. Hu^{35b}, Y. Huang⁴⁴, Z. Hubacek¹²⁹, F. Hubaut⁸⁷, F. Huegging²³, T.B. Huffman¹²¹, E.W. Hughes³⁷, G. Hughes⁷⁴, M. Huhtinen³², T.A. Hülsing⁸⁵, P. Huo¹⁴⁹, N. Huseynov^{67,b}, J. Huston⁹², J. Huth⁵⁹, G. Iacobucci⁵¹, G. Iakovidis²⁷,

I. Ibragimov¹⁴², L. Iconomidou-Fayard¹¹⁸, E. Ideal¹⁷⁶, Z. Idrissi^{136e}, P. Iengo³², O. Igonkina¹⁰⁸,
 T. Iizawa¹⁷¹, Y. Ikegami⁶⁸, M. Ikeno⁶⁸, Y. Ilchenko^{11,t}, D. Iliadis¹⁵⁵, N. Ilic¹⁴⁴, T. Ince¹⁰²,
 G. Introzzi^{122a,122b}, P. Ioannou^{9,*}, M. Iodice^{135a}, K. Iordanidou³⁷, V. Ippolito⁵⁹, M. Ishino⁷⁰,
 M. Ishitsuka¹⁵⁸, R. Ishmukhametov¹¹², C. Issever¹²¹, S. Isti^{20a}, F. Ito¹⁶¹, J.M. Iturbe Ponce⁸⁶,
 R. Iuppa^{134a,134b}, W. Iwanski⁴¹, H. Iwasaki⁶⁸, J.M. Izen⁴³, V. Izzo^{105a}, S. Jabbar³, B. Jackson¹²³,
 M. Jackson⁷⁶, P. Jackson¹, V. Jain², K.B. Jakobi⁸⁵, K. Jakobs⁵⁰, S. Jakobsen³², T. Jakoubek¹²⁸,
 D.O. Jamin¹¹⁵, D.K. Jana⁸¹, E. Jansen⁸⁰, R. Jansky⁶⁴, J. Janssen²³, M. Janus⁵⁶, G. Jarlskog⁸³,
 N. Javadov^{67,b}, T. Javurek⁵⁰, F. Jeanneau¹³⁷, L. Jeanty¹⁶, J. Jejelava^{53a,u}, G.-Y. Jeng¹⁵¹, D. Jennens⁹⁰,
 P. Jenni^{50,v}, J. Jentzsch⁴⁵, C. Jeske¹⁷⁰, S. Jézéquel⁵, H. Ji¹⁷³, J. Jia¹⁴⁹, H. Jiang⁶⁶, Y. Jiang^{35b},
 S. Jiggins⁸⁰, J. Jimenez Pena¹⁶⁷, S. Jin^{35a}, A. Jinaru^{28b}, O. Jinnouchi¹⁵⁸, P. Johansson¹⁴⁰, K.A. Johns⁷,
 W.J. Johnson¹³⁹, K. Jon-And^{147a,147b}, G. Jones¹⁷⁰, R.W.L. Jones⁷⁴, S. Jones⁷, T.J. Jones⁷⁶,
 J. Jongmanns^{60a}, P.M. Jorge^{127a,127b}, J. Jovicevic^{160a}, X. Ju¹⁷³, A. Juste Rozas^{13,q}, M.K. Köhler¹⁷²,
 A. Kaczmarcka⁴¹, M. Kado¹¹⁸, H. Kagan¹¹², M. Kagan¹⁴⁴, S.J. Kahn⁸⁷, E. Kajomovitz⁴⁷,
 C.W. Kalderon¹²¹, A. Kaluza⁸⁵, S. Kama⁴², A. Kamenshchikov¹³¹, N. Kanaya¹⁵⁶, S. Kaneti³⁰,
 L. Kanjur⁷⁷, V.A. Kantserov⁹⁹, J. Kanzaki⁶⁸, B. Kaplan¹¹¹, L.S. Kaplan¹⁷³, A. Kapliy³³, D. Kar^{146c},
 K. Karakostas¹⁰, A. Karamaoun³, N. Karastathis¹⁰, M.J. Kareem⁵⁶, E. Karentzos¹⁰, M. Karnevskiy⁸⁵,
 S.N. Karpov⁶⁷, Z.M. Karpova⁶⁷, K. Karthik¹¹¹, V. Kartvelishvili⁷⁴, A.N. Karyukhin¹³¹, K. Kasahara¹⁶¹,
 L. Kashif¹⁷³, R.D. Kass¹¹², A. Kastanas¹⁵, Y. Kataoka¹⁵⁶, C. Kato¹⁵⁶, A. Katre⁵¹, J. Katzy⁴⁴,
 K. Kawagoe⁷², T. Kawamoto¹⁵⁶, G. Kawamura⁵⁶, S. Kazama¹⁵⁶, V.F. Kazanin^{110,c}, R. Keeler¹⁶⁹,
 R. Kehoe⁴², J.S. Keller⁴⁴, J.J. Kempster⁷⁹, K. Kentaro¹⁰⁴, H. Keoshkerian¹⁵⁹, O. Kepka¹²⁸,
 B.P. Kerševan⁷⁷, S. Kersten¹⁷⁵, R.A. Keyes⁸⁹, F. Khalil-zada¹², A. Khanov¹¹⁵, A.G. Kharlamov^{110,c},
 T.J. Khoo⁵¹, V. Khovanskij⁹⁸, E. Khramov⁶⁷, J. Khubua^{53b,w}, S. Kido⁶⁹, H.Y. Kim⁸, S.H. Kim¹⁶¹,
 Y.K. Kim³³, N. Kimura¹⁵⁵, O.M. Kind¹⁷, B.T. King⁷⁶, M. King¹⁶⁷, S.B. King¹⁶⁸, J. Kirk¹³²,
 A.E. Kiryunin¹⁰², T. Kishimoto⁶⁹, D. Kisielewska^{40a}, F. Kiss⁵⁰, K. Kiuchi¹⁶¹, O. Kivernyk¹³⁷,
 E. Kladiva^{145b}, M.H. Klein³⁷, M. Klein⁷⁶, U. Klein⁷⁶, K. Kleinknecht⁸⁵, P. Klimek^{147a,147b},
 A. Klimentov²⁷, R. Klingenberg⁴⁵, J.A. Klinger¹⁴⁰, T. Klioutchnikova³², E.-E. Kluge^{60a}, P. Kluit¹⁰⁸,
 S. Kluth¹⁰², J. Knapik⁴¹, E. Kneringer⁶⁴, E.B.F.G. Knoops⁸⁷, A. Knue⁵⁵, A. Kobayashi¹⁵⁶,
 D. Kobayashi¹⁵⁸, T. Kobayashi¹⁵⁶, M. Kobel⁴⁶, M. Kocian¹⁴⁴, P. Kodys¹³⁰, T. Koffman³¹, E. Koffeman¹⁰⁸,
 T. Koi¹⁴⁴, H. Kolanoski¹⁷, M. Kolb^{60b}, I. Koletsou⁵, A.A. Komar^{97,*}, Y. Komori¹⁵⁶, T. Kondo⁶⁸,
 N. Kondrashova⁴⁴, K. Köneke⁵⁰, A.C. König¹⁰⁷, T. Kono^{68,x}, R. Konoplich^{111,y}, N. Konstantinidis⁸⁰,
 R. Kopeliansky⁶³, S. Koperny^{40a}, L. Köpke⁸⁵, A.K. Kopp⁵⁰, K. Korcyl⁴¹, K. Kordas¹⁵⁵, A. Korn⁸⁰,
 A.A. Korol^{110,c}, I. Korolkov¹³, E.V. Korolkova¹⁴⁰, O. Kortner¹⁰², S. Kortner¹⁰², T. Kosek¹³⁰,
 V.V. Kostyukhin²³, A. Kotwal⁴⁷, A. Kourkoumeli-Charalampidi¹⁵⁵, C. Kourkoumelis⁹, V. Kouskoura²⁷,
 A.B. Kowalewska⁴¹, R. Kowalewski¹⁶⁹, T.Z. Kowalski^{40a}, C. Kozakai¹⁵⁶, W. Kozanecki¹³⁷,
 A.S. Kozhin¹³¹, V.A. Kramarenko¹⁰⁰, G. Kramberger⁷⁷, D. Krasnopol'tsev⁹⁹, M.W. Krasny⁸²,
 A. Krasznahorkay³², J.K. Kraus²³, A. Kravchenko²⁷, M. Kretz^{60c}, J. Kretzscher⁷⁶, K. Kreutzfeldt⁵⁴,
 P. Krieger¹⁵⁹, K. Krizka³³, K. Kroeninger⁴⁵, H. Kroha¹⁰², J. Kroll¹²³, J. Kroeseberg²³, J. Krstic¹⁴,
 U. Kruchonak⁶⁷, H. Krüger²³, N. Krumnack⁶⁶, A. Kruse¹⁷³, M.C. Kruse⁴⁷, M. Kruskal²⁴, T. Kubota⁹⁰,
 H. Kucuk⁸⁰, S. Kuday^{4b}, J.T. Kuechler¹⁷⁵, S. Kuehn⁵⁰, A. Kugel^{60c}, F. Kuger¹⁷⁴, A. Kuhl¹³⁸, T. Kuhl⁴⁴,
 V. Kukhtin⁶⁷, R. Kukla¹³⁷, Y. Kulchitsky⁹⁴, S. Kuleshov^{34b}, M. Kuna^{133a,133b}, T. Kunigo⁷⁰, A. Kupco¹²⁸,
 H. Kurashige⁶⁹, Y.A. Kurochkin⁹⁴, V. Kus¹²⁸, E.S. Kuwertz¹⁶⁹, M. Kuze¹⁵⁸, J. Kvita¹¹⁶, T. Kwan¹⁶⁹,
 D. Kyriazopoulos¹⁴⁰, A. La Rosa¹⁰², J.L. La Rosa Navarro^{26d}, L. La Rotonda^{39a,39b}, C. Lacasta¹⁶⁷,
 F. Lacava^{133a,133b}, J. Lacey³¹, H. Lacker¹⁷, D. Lacour⁸², V.R. Lacuesta¹⁶⁷, E. Ladygin⁶⁷, R. Lafaye⁵,
 B. Laforge⁸², T. Lagouri¹⁷⁶, S. Lai⁵⁶, S. Lammers⁶³, W. Lampl⁷, E. Lançon¹³⁷, U. Landgraf⁵⁰,
 M.P.J. Landon⁷⁸, V.S. Lang^{60a}, J.C. Lange¹³, A.J. Lankford¹⁶³, F. Lanni²⁷, K. Lantzsch²³, A. Lanza^{122a},
 S. Laplace⁸², C. Lapoire³², J.F. Laporte¹³⁷, T. Lari^{93a}, F. Lasagni Manghi^{22a,22b}, M. Lassnig³²,
 P. Laurelli⁴⁹, W. Lavrijssen¹⁶, A.T. Law¹³⁸, P. Laycock⁷⁶, T. Lazovich⁵⁹, M. Lazzaroni^{93a,93b}, B. Le⁹⁰,

O. Le Dertz⁸², E. Le Guiriec⁸⁷, E.P. Le Quilleuc¹³⁷, M. LeBlanc¹⁶⁹, T. LeCompte⁶,
 F. Ledroit-Guillon⁵⁷, C.A. Lee²⁷, S.C. Lee¹⁵², L. Lee¹, G. Lefebvre⁸², M. Lefebvre¹⁶⁹, F. Legger¹⁰¹,
 C. Leggett¹⁶, A. Lehan⁷⁶, G. Lehmann Miotto³², X. Lei⁷, W.A. Leight³¹, A. Leisos^{155,z}, A.G. Leister¹⁷⁶,
 M.A.L. Leite^{26d}, R. Leitner¹³⁰, D. Lellouch¹⁷², B. Lemmer⁵⁶, K.J.C. Leney⁸⁰, T. Lenz²³, B. Lenzi³²,
 R. Leone⁷, S. Leone^{125a,125b}, C. Leonidopoulos⁴⁸, S. Leontsinis¹⁰, G. Lerner¹⁵⁰, C. Leroy⁹⁶,
 A.A.J. Lesage¹³⁷, C.G. Lester³⁰, M. Levchenko¹²⁴, J. Levêque⁵, D. Levin⁹¹, L.J. Levinson¹⁷²,
 M. Levy¹⁹, D. Lewis⁷⁸, A.M. Leyko²³, M. Leyton⁴³, B. Li^{35b,aa}, H. Li¹⁴⁹, H.L. Li³³, L. Li⁴⁷, L. Li^{35e},
 Q. Li^{35a}, S. Li⁴⁷, X. Li⁸⁶, Y. Li¹⁴², Z. Liang^{35a}, B. Liberti^{134a}, A. Liblong¹⁵⁹, P. Lichard³², K. Lie¹⁶⁶,
 J. Liebal²³, W. Liebig¹⁵, A. Limosani¹⁵¹, S.C. Lin^{152,ab}, T.H. Lin⁸⁵, B.E. Lindquist¹⁴⁹, A.E. Lioni⁵¹,
 E. Lipeles¹²³, A. Lipniacka¹⁵, M. Lisovyi^{60b}, T.M. Liss¹⁶⁶, A. Lister¹⁶⁸, A.M. Litke¹³⁸, B. Liu^{152,ac},
 D. Liu¹⁵², H. Liu⁹¹, H. Liu²⁷, J. Liu⁸⁷, J.B. Liu^{35b}, K. Liu⁸⁷, L. Liu¹⁶⁶, M. Liu⁴⁷, M. Liu^{35b}, Y.L. Liu^{35b},
 Y. Liu^{35b}, M. Livan^{122a,122b}, A. Lleres⁵⁷, J. Llorente Merino^{35a}, S.L. Lloyd⁷⁸, F. Lo Sterzo¹⁵²,
 E. Lobodzinska⁴⁴, P. Loch⁷, W.S. Lockman¹³⁸, F.K. Loebinger⁸⁶, A.E. Loevschall-Jensen³⁸,
 K.M. Loew²⁵, A. Loginov¹⁷⁶, T. Lohse¹⁷, K. Lohwasser⁴⁴, M. Lokajicek¹²⁸, B.A. Long²⁴, J.D. Long¹⁶⁶,
 R.E. Long⁷⁴, L. Longo^{75a,75b}, K.A.Looper¹¹², L. Lopes^{127a}, D. Lopez Mateos⁵⁹, B. Lopez Paredes¹⁴⁰,
 I. Lopez Paz¹³, A. Lopez Solis⁸², J. Lorenz¹⁰¹, N. Lorenzo Martinez⁶³, M. Losada²¹, P.J. Lösel¹⁰¹,
 X. Lou^{35a}, A. Lounis¹¹⁸, J. Love⁶, P.A. Love⁷⁴, H. Lu^{62a}, N. Lu⁹¹, H.J. Lubatti¹³⁹, C. Luci^{133a,133b},
 A. Lucotte⁵⁷, C. Luedtke⁵⁰, F. Luehring⁶³, W. Lukas⁶⁴, L. Luminari^{133a}, O. Lundberg^{147a,147b},
 B. Lund-Jensen¹⁴⁸, P.M. Luzi⁸², D. Lynn²⁷, R. Lysak¹²⁸, E. Lytken⁸³, V. Lyubushkin⁶⁷, H. Ma²⁷,
 L.L. Ma^{35d}, Y. Ma^{35d}, G. Maccarrone⁴⁹, A. Macchiolo¹⁰², C.M. Macdonald¹⁴⁰, B. Maček⁷⁷,
 J. Machado Miguens^{123,127b}, D. Madaffari⁸⁷, R. Madar³⁶, H.J. Maddocks¹⁶⁵, W.F. Mader⁴⁶,
 A. Madsen⁴⁴, J. Maeda⁶⁹, S. Maeland¹⁵, T. Maeno²⁷, A. Maevskiy¹⁰⁰, E. Magradze⁵⁶, J. Mahlstedt¹⁰⁸,
 C. Maiani¹¹⁸, C. Maidantchik^{26a}, A.A. Maier¹⁰², T. Maier¹⁰¹, A. Maio^{127a,127b,127d}, S. Majewski¹¹⁷,
 Y. Makida⁶⁸, N. Makovec¹¹⁸, B. Malaescu⁸², Pa. Malecki⁴¹, V.P. Maleev¹²⁴, F. Malek⁵⁷, U. Mallik⁶⁵,
 D. Malon⁶, C. Malone¹⁴⁴, S. Maltezos¹⁰, V.M. Malyshev¹¹⁰, S. Malyukov³², J. Mamuzic¹⁶⁷,
 G. Mancini⁴⁹, B. Mandelli³², L. Mandelli^{93a}, I. Mandić⁷⁷, J. Maneira^{127a,127b},
 L. Manhaes de Andrade Filho^{26b}, J. Manjarres Ramos^{160b}, A. Mann¹⁰¹, A. Manousos³²,
 B. Mansoulie¹³⁷, J.D. Mansour^{35a}, R. Mantifel⁸⁹, M. Mantoani⁵⁶, S. Manzoni^{93a,93b}, L. Mapelli³²,
 G. Marceca²⁹, L. March⁵¹, G. Marchiori⁸², M. Marcisovsky¹²⁸, M. Marjanovic¹⁴, D.E. Marley⁹¹,
 F. Marroquim^{26a}, S.P. Marsden⁸⁶, Z. Marshall¹⁶, S. Marti-Garcia¹⁶⁷, B. Martin⁹², T.A. Martin¹⁷⁰,
 V.J. Martin⁴⁸, B. Martin dit Latour¹⁵, M. Martinez^{13,q}, S. Martin-Haugh¹³², V.S. Martoiu^{28b},
 A.C. Martyniuk⁸⁰, M. Marx¹³⁹, A. Marzin³², L. Masetti⁸⁵, T. Mashimo¹⁵⁶, R. Mashinistov⁹⁷, J. Masik⁸⁶,
 A.L. Maslennikov^{110,c}, I. Massa^{22a,22b}, L. Massa^{22a,22b}, P. Mastrandrea⁵, A. Mastroberardino^{39a,39b},
 T. Masubuchi¹⁵⁶, P. Mättig¹⁷⁵, J. Mattmann⁸⁵, J. Maurer^{28b}, S.J. Maxfield⁷⁶, D.A. Maximov^{110,c},
 R. Mazini¹⁵², S.M. Mazza^{93a,93b}, N.C. Mc Fadden¹⁰⁶, G. Mc Goldrick¹⁵⁹, S.P. Mc Kee⁹¹, A. McCarn⁹¹,
 R.L. McCarthy¹⁴⁹, T.G. McCarthy¹⁰², L.I. McClymont⁸⁰, E.F. McDonald⁹⁰, K.W. McFarlane^{58,*},
 J.A. McFayden⁸⁰, G. Mchedlidze⁵⁶, S.J. McMahon¹³², R.A. McPherson^{169,l}, M. Medinnis⁴⁴,
 S. Meehan¹³⁹, S. Mehlhase¹⁰¹, A. Mehta⁷⁶, K. Meier^{60a}, C. Meineck¹⁰¹, B. Meirose⁴³, D. Melini¹⁶⁷,
 B.R. Mellado Garcia^{146c}, M. Melo^{145a}, F. Meloni¹⁸, A. Mengarelli^{22a,22b}, S. Menke¹⁰², E. Meoni¹⁶²,
 S. Mergelmeyer¹⁷, P. Mermod⁵¹, L. Merola^{105a,105b}, C. Meroni^{93a}, F.S. Merritt³³, A. Messina^{133a,133b},
 J. Metcalfe⁶, A.S. Mete¹⁶³, C. Meyer⁸⁵, C. Meyer¹²³, J.-P. Meyer¹³⁷, J. Meyer¹⁰⁸,
 H. Meyer Zu Theenhausen^{60a}, F. Miano¹⁵⁰, R.P. Middleton¹³², S. Miglioranzi^{52a,52b}, L. Mijović²³,
 G. Mikenberg¹⁷², M. Mikestikova¹²⁸, M. Mikuž⁷⁷, M. Milesi⁹⁰, A. Milic⁶⁴, D.W. Miller³³, C. Mills⁴⁸,
 A. Milov¹⁷², D.A. Milstead^{147a,147b}, A.A. Minaenko¹³¹, Y. Minami¹⁵⁶, I.A. Minashvili⁶⁷, A.I. Mincer¹¹¹,
 B. Mindur^{40a}, M. Mineev⁶⁷, Y. Ming¹⁷³, L.M. Mir¹³, K.P. Mistry¹²³, T. Mitani¹⁷¹, J. Mitrevski¹⁰¹,
 V.A. Mitsou¹⁶⁷, A. Miucci⁵¹, P.S. Miyagawa¹⁴⁰, J.U. Mjörnmark⁸³, T. Moa^{147a,147b}, K. Mochizuki⁹⁶,
 S. Mohapatra³⁷, S. Molander^{147a,147b}, R. Moles-Valls²³, R. Monden⁷⁰, M.C. Mondragon⁹², K. Mönig⁴⁴,

J. Monk³⁸, E. Monnier⁸⁷, A. Montalbano¹⁴⁹, J. Montejo Berlingen³², F. Monticelli⁷³, S. Monzani^{93a,93b}, R.W. Moore³, N. Morange¹¹⁸, D. Moreno²¹, M. Moreno Llácer⁵⁶, P. Morettini^{52a}, D. Mori¹⁴³, T. Mori¹⁵⁶, M. Morii⁵⁹, M. Morinaga¹⁵⁶, V. Morisbak¹²⁰, S. Moritz⁸⁵, A.K. Morley¹⁵¹, G. Mornacchi³², J.D. Morris⁷⁸, S.S. Mortensen³⁸, L. Morvaj¹⁴⁹, M. Mosidze^{53b}, J. Moss¹⁴⁴, K. Motohashi¹⁵⁸, R. Mount¹⁴⁴, E. Mountricha²⁷, S.V. Mouraviev^{97,*}, E.J.W. Moyse⁸⁸, S. Muanza⁸⁷, R.D. Mudd¹⁹, F. Mueller¹⁰², J. Mueller¹²⁶, R.S.P. Mueller¹⁰¹, T. Mueller³⁰, D. Muenstermann⁷⁴, P. Mullen⁵⁵, G.A. Mullier¹⁸, D.P. Mungo^{93a,93b}, F.J. Munoz Sanchez⁸⁶, J.A. Murillo Quijada¹⁹, W.J. Murray^{170,132}, H. Musheghyan⁵⁶, M. Muskinja⁷⁷, A.G. Myagkov^{131,ad}, M. Myska¹²⁹, B.P. Nachman¹⁴⁴, O. Nackenhorst⁵¹, K. Nagai¹²¹, R. Nagai^{68,x}, K. Nagano⁶⁸, Y. Nagasaka⁶¹, K. Nagata¹⁶¹, M. Nagel⁵⁰, E. Nagy⁸⁷, A.M. Nairz³², Y. Nakahama³², K. Nakamura⁶⁸, T. Nakamura¹⁵⁶, I. Nakano¹¹³, H. Namasivayam⁴³, R.F. Naranjo Garcia⁴⁴, R. Narayan¹¹, D.I. Narrias Villar^{60a}, I. Naryshkin¹²⁴, T. Naumann⁴⁴, G. Navarro²¹, R. Nayyar⁷, H.A. Neal⁹¹, P.Yu. Nechaeva⁹⁷, T.J. Neep⁸⁶, P.D. Nef¹⁴⁴, A. Negri^{122a,122b}, M. Negrini^{22a}, S. Nektarijevic¹⁰⁷, C. Nellist¹¹⁸, A. Nelson¹⁶³, S. Nemecek¹²⁸, P. Nemethy¹¹¹, A.A. Nepomuceno^{26a}, M. Nessi^{32,ae}, M.S. Neubauer¹⁶⁶, M. Neumann¹⁷⁵, R.M. Neves¹¹¹, P. Nevski²⁷, P.R. Newman¹⁹, D.H. Nguyen⁶, T. Nguyen Manh⁹⁶, R.B. Nickerson¹²¹, R. Nicolaïdou¹³⁷, J. Nielsen¹³⁸, A. Nikiforov¹⁷, V. Nikolaenko^{131,ad}, I. Nikolic-Audit⁸², K. Nikolopoulos¹⁹, J.K. Nilsen¹²⁰, P. Nilsson²⁷, Y. Ninomiya¹⁵⁶, A. Nisati^{133a}, R. Nisius¹⁰², T. Nobe¹⁵⁶, L. Nodulman⁶, M. Nomachi¹¹⁹, I. Nomidis³¹, T. Nooney⁷⁸, S. Norberg¹¹⁴, M. Nordberg³², N. Norjoharuddeen¹²¹, O. Novgorodova⁴⁶, S. Nowak¹⁰², M. Nozaki⁶⁸, L. Nozka¹¹⁶, K. Ntekas¹⁰, E. Nurse⁸⁰, F. Nuti⁹⁰, F. O'grady⁷, D.C. O'Neil¹⁴³, A.A. O'Rourke⁴⁴, V. O'Shea⁵⁵, F.G. Oakham^{31,d}, H. Oberlack¹⁰², T. Obermann²³, J. Ocariz⁸², A. Ochi⁶⁹, I. Ochoa³⁷, J.P. Ochoa-Ricoux^{34a}, S. Oda⁷², S. Odaka⁶⁸, H. Ogren⁶³, A. Oh⁸⁶, S.H. Oh⁴⁷, C.C. Ohm¹⁶, H. Ohman¹⁶⁵, H. Oide³², H. Okawa¹⁶¹, Y. Okumura³³, T. Okuyama⁶⁸, A. Olariu^{28b}, L.F. Oleiro Seabra^{127a}, S.A. Olivares Pino⁴⁸, D. Oliveira Damazio²⁷, A. Olszewski⁴¹, J. Olszowska⁴¹, A. Onofre^{127a,127e}, K. Onogi¹⁰⁴, P.U.E. Onyisi^{11,t}, M.J. Oreglia³³, Y. Oren¹⁵⁴, D. Orestano^{135a,135b}, N. Orlando^{62b}, R.S. Orr¹⁵⁹, B. Osculati^{52a,52b}, R. Ospanov⁸⁶, G. Otero y Garzon²⁹, H. Otono⁷², M. Ouchrif^{136d}, F. Ould-Saada¹²⁰, A. Ouraou¹³⁷, K.P. Oussoren¹⁰⁸, Q. Ouyang^{35a}, M. Owen⁵⁵, R.E. Owen¹⁹, V.E. Ozcan^{20a}, N. Ozturk⁸, K. Pachal¹⁴³, A. Pacheco Pages¹³, C. Padilla Aranda¹³, M. Pagáčová⁵⁰, S. Pagan Griso¹⁶, F. Paige²⁷, P. Pais⁸⁸, K. Pajchel¹²⁰, G. Palacino^{160b}, S. Palestini³², M. Palka^{40b}, D. Pallin³⁶, A. Palma^{127a,127b}, E.St. Panagiotopoulou¹⁰, C.E. Pandini⁸², J.G. Panduro Vazquez⁷⁹, P. Pani^{147a,147b}, S. Panitkin²⁷, D. Pantea^{28b}, L. Paolozzi⁵¹, Th.D. Papadopoulou¹⁰, K. Papageorgiou¹⁵⁵, A. Paramonov⁶, D. Paredes Hernandez¹⁷⁶, A.J. Parker⁷⁴, M.A. Parker³⁰, K.A. Parker¹⁴⁰, F. Parodi^{52a,52b}, J.A. Parsons³⁷, U. Parzefall⁵⁰, V.R. Pascuzzi¹⁵⁹, E. Pasqualucci^{133a}, S. Passaggio^{52a}, Fr. Pastore⁷⁹, G. Pásztor^{31,af}, S. Pataraia¹⁷⁵, J.R. Pater⁸⁶, T. Pauly³², J. Pearce¹⁶⁹, B. Pearson¹¹⁴, L.E. Pedersen³⁸, M. Pedersen¹²⁰, S. Pedraza Lopez¹⁶⁷, R. Pedro^{127a,127b}, S.V. Peleganchuk^{110,c}, D. Pelikan¹⁶⁵, O. Penc¹²⁸, C. Peng^{35a}, H. Peng^{35b}, J. Penwell⁶³, B.S. Peralva^{26b}, M.M. Perego¹³⁷, D.V. Perepelitsa²⁷, E. Perez Codina^{160a}, L. Perini^{93a,93b}, H. Pernegger³², S. Perrella^{105a,105b}, R. Peschke⁴⁴, V.D. Peshekhanov⁶⁷, K. Peters⁴⁴, R.F.Y. Peters⁸⁶, B.A. Petersen³², T.C. Petersen³⁸, E. Petit⁵⁷, A. Petridis¹, C. Petridou¹⁵⁵, P. Petroff¹¹⁸, E. Petrolo^{133a}, M. Petrov¹²¹, F. Petrucci^{135a,135b}, N.E. Pettersson⁸⁸, A. Peyaud¹³⁷, R. Pezoa^{34b}, P.W. Phillips¹³², G. Piacquadio¹⁴⁴, E. Pianori¹⁷⁰, A. Picazio⁸⁸, E. Piccaro⁷⁸, M. Piccinini^{22a,22b}, M.A. Pickering¹²¹, R. Piegaia²⁹, J.E. Pilcher³³, A.D. Pilkington⁸⁶, A.W.J. Pin⁸⁶, M. Pinamonti^{164a,164c,ag}, J.L. Pinfold³, A. Pingel³⁸, S. Pires⁸², H. Pirumov⁴⁴, M. Pitt¹⁷², L. Plazak^{145a}, M.-A. Pleier²⁷, V. Pleskot⁸⁵, E. Plotnikova⁶⁷, P. Plucinski⁹², D. Pluth⁶⁶, R. Poettgen^{147a,147b}, L. Poggioli¹¹⁸, D. Pohl²³, G. Polesello^{122a}, A. Poley⁴⁴, A. Policicchio^{39a,39b}, R. Polifka¹⁵⁹, A. Polini^{22a}, C.S. Pollard⁵⁵, V. Polychronakos²⁷, K. Pommès³², L. Pontecorvo^{133a}, B.G. Pope⁹², G.A. Popeneciu^{28c}, D.S. Popovic¹⁴, A. Poppleton³², S. Pospisil¹²⁹, K. Potamianos¹⁶, I.N. Potrap⁶⁷, C.J. Potter³⁰, C.T. Potter¹¹⁷, G. Pouillard³², J. Poveda³², V. Pozdnyakov⁶⁷, M.E. Pozo Astigarraga³², P. Pralavorio⁸⁷, A. Pranko¹⁶, S. Prell⁶⁶, D. Price⁸⁶,

L.E. Price⁶, M. Primavera^{75a}, S. Prince⁸⁹, M. Proissl⁴⁸, K. Prokofiev^{62c}, F. Prokoshin^{34b},
 S. Protopopescu²⁷, J. Proudfoot⁶, M. Przybycien^{40a}, D. Puddu^{135a,135b}, M. Purohit^{27,ah}, P. Puzo¹¹⁸,
 J. Qian⁹¹, G. Qin⁵⁵, Y. Qin⁸⁶, A. Quadt⁵⁶, W.B. Quayle^{164a,164b}, M. Queitsch-Maitland⁸⁶, D. Quilty⁵⁵,
 S. Raddum¹²⁰, V. Radeka²⁷, V. Radescu^{60b}, S.K. Radhakrishnan¹⁴⁹, P. Radloff¹¹⁷, P. Rados⁹⁰,
 F. Ragusa^{93a,93b}, G. Rahal¹⁷⁸, J.A. Raine⁸⁶, S. Rajagopalan²⁷, M. Rammensee³², C. Rangel-Smith¹⁶⁵,
 M.G. Ratti^{93a,93b}, F. Rauscher¹⁰¹, S. Rave⁸⁵, T. Ravenscroft⁵⁵, I. Ravinovich¹⁷², M. Raymond³²,
 A.L. Read¹²⁰, N.P. Readioff⁷⁶, M. Reale^{75a,75b}, D.M. Rebuzzi^{122a,122b}, A. Redelbach¹⁷⁴, G. Redlinger²⁷,
 R. Reece¹³⁸, K. Reeves⁴³, L. Rehnisch¹⁷, J. Reichert¹²³, H. Reisin²⁹, C. Rembsler³², H. Ren^{35a},
 M. Rescigno^{133a}, S. Resconi^{93a}, O.L. Rezanova^{110,c}, P. Reznicek¹³⁰, R. Rezvani⁹⁶, R. Richter¹⁰²,
 S. Richter⁸⁰, E. Richter-Was^{40b}, O. Ricken²³, M. Ridel⁸², P. Rieck¹⁷, C.J. Riegel¹⁷⁵, J. Rieger⁵⁶,
 O. Rifki¹¹⁴, M. Rijssenbeek¹⁴⁹, A. Rimoldi^{122a,122b}, M. Rimoldi¹⁸, L. Rinaldi^{22a}, B. Ristic⁵¹, E. Ritsch³²,
 I. Riu¹³, F. Rizatdinova¹¹⁵, E. Rizvi⁷⁸, C. Rizzi¹³, S.H. Robertson^{89,l}, A. Robichaud-Veronneau⁸⁹,
 D. Robinson³⁰, J.E.M. Robinson⁴⁴, A. Robson⁵⁵, C. Roda^{125a,125b}, Y. Rodina⁸⁷, A. Rodriguez Perez¹³,
 D. Rodriguez Rodriguez¹⁶⁷, S. Roe³², C.S. Rogan⁵⁹, O. Røhne¹²⁰, A. Romaniouk⁹⁹, M. Romano^{22a,22b},
 S.M. Romano Saez³⁶, E. Romero Adam¹⁶⁷, N. Rompotis¹³⁹, M. Ronzani⁵⁰, L. Roos⁸², E. Ros¹⁶⁷,
 S. Rosati^{133a}, K. Rosbach⁵⁰, P. Rose¹³⁸, O. Rosenthal¹⁴², N.-A. Rosien⁵⁶, V. Rossetti^{147a,147b},
 E. Rossi^{105a,105b}, L.P. Rossi^{52a}, J.H.N. Rosten³⁰, R. Rosten¹³⁹, M. Rotaru^{28b}, I. Roth¹⁷², J. Rothberg¹³⁹,
 D. Rousseau¹¹⁸, C.R. Royon¹³⁷, A. Rozanov⁸⁷, Y. Rozen¹⁵³, X. Ruan^{146c}, F. Rubbo¹⁴⁴,
 M.S. Rudolph¹⁵⁹, F. Rühr⁵⁰, A. Ruiz-Martinez³¹, Z. Rurikova⁵⁰, N.A. Rusakovich⁶⁷, A. Ruschke¹⁰¹,
 H.L. Russell¹³⁹, J.P. Rutherford⁷, N. Ruthmann³², Y.F. Ryabov¹²⁴, M. Rybar¹⁶⁶, G. Rybkin¹¹⁸, S. Ryu⁶,
 A. Ryzhov¹³¹, G.F. Rzehorz⁵⁶, A.F. Saavedra¹⁵¹, G. Sabato¹⁰⁸, S. Sacerdoti²⁹, H.F-W. Sadrozinski¹³⁸,
 R. Sadykov⁶⁷, F. Safai Tehrani^{133a}, P. Saha¹⁰⁹, M. Sahinsoy^{60a}, M. Saimpert¹³⁷, T. Saito¹⁵⁶,
 H. Sakamoto¹⁵⁶, Y. Sakurai¹⁷¹, G. Salamanna^{135a,135b}, A. Salamon^{134a,134b}, J.E. Salazar Loyola^{34b},
 D. Salek¹⁰⁸, P.H. Sales De Bruin¹³⁹, D. Salihagic¹⁰², A. Salnikov¹⁴⁴, J. Salt¹⁶⁷, D. Salvatore^{39a,39b},
 F. Salvatore¹⁵⁰, A. Salvucci^{62a}, A. Salzburger³², D. Sammel⁵⁰, D. Sampsonidis¹⁵⁵, A. Sanchez^{105a,105b},
 J. Sánchez¹⁶⁷, V. Sanchez Martinez¹⁶⁷, H. Sandaker¹²⁰, R.L. Sandbach⁷⁸, H.G. Sander⁸⁵,
 M. Sandhoff¹⁷⁵, C. Sandoval²¹, R. Sandstroem¹⁰², D.P.C. Sankey¹³², M. Sannino^{52a,52b}, A. Sansoni⁴⁹,
 C. Santoni³⁶, R. Santonico^{134a,134b}, H. Santos^{127a}, I. Santoyo Castillo¹⁵⁰, K. Sapp¹²⁶, A. Sapronov⁶⁷,
 J.G. Saraiva^{127a,127d}, B. Sarrazin²³, O. Sasaki⁶⁸, Y. Sasaki¹⁵⁶, K. Sato¹⁶¹, G. Sauvage^{5,*}, E. Sauvan⁵,
 G. Savage⁷⁹, P. Savard^{159,d}, C. Sawyer¹³², L. Sawyer^{81,p}, J. Saxon³³, C. Sbarra^{22a}, A. Sbrizzi^{22a,22b},
 T. Scanlon⁸⁰, D.A. Scannicchio¹⁶³, M. Scarcella¹⁵¹, V. Scarfone^{39a,39b}, J. Schaarschmidt¹⁷²,
 P. Schacht¹⁰², B.M. Schachtner¹⁰¹, D. Schaefer³², R. Schaefer⁴⁴, J. Schaeffer⁸⁵, S. Schaepe²³,
 S. Schaetzl^{60b}, U. Schäfer⁸⁵, A.C. Schaffer¹¹⁸, D. Schaille¹⁰¹, R.D. Schamberger¹⁴⁹, V. Scharf^{60a},
 V.A. Schegelsky¹²⁴, D. Scheirich¹³⁰, M. Schernau¹⁶³, C. Schiavi^{52a,52b}, S. Schier¹³⁸, C. Schillo⁵⁰,
 M. Schioppa^{39a,39b}, S. Schlenker³², K.R. Schmidt-Sommerfeld¹⁰², K. Schmieden³², C. Schmitt⁸⁵,
 S. Schmitt⁴⁴, S. Schmitz⁸⁵, B. Schneider^{160a}, U. Schnoor⁵⁰, L. Schoeffel¹³⁷, A. Schoening^{60b},
 B.D. Schoenrock⁹², E. Schopf²³, M. Schott⁸⁵, J. Schovancova⁸, S. Schramm⁵¹, M. Schreyer¹⁷⁴,
 N. Schuh⁸⁵, M.J. Schultens²³, H.-C. Schultz-Coulon^{60a}, H. Schulz¹⁷, M. Schumacher⁵⁰,
 B.A. Schumm¹³⁸, Ph. Schune¹³⁷, A. Schwartzman¹⁴⁴, T.A. Schwarz⁹¹, Ph. Schwegler¹⁰²,
 H. Schweiger⁸⁶, Ph. Schwemling¹³⁷, R. Schwienhorst⁹², J. Schwindling¹³⁷, T. Schwindt²³, G. Sciolla²⁵,
 F. Scuri^{125a,125b}, F. Scutti⁹⁰, J. Searcy⁹¹, P. Seema²³, S.C. Seidel¹⁰⁶, A. Seiden¹³⁸, F. Seifert¹²⁹,
 J.M. Seixas^{26a}, G. Sekhniaidze^{105a}, K. Sekhon⁹¹, S.J. Sekula⁴², D.M. Seliverstov^{124,*},
 N. Semprini-Cesari^{22a,22b}, C. Serfon¹²⁰, L. Serin¹¹⁸, L. Serkin^{164a,164b}, M. Sessa^{135a,135b}, R. Seuster¹⁶⁹,
 H. Severini¹¹⁴, T. Sfiligoj⁷⁷, F. Sforza³², A. Sfyrla⁵¹, E. Shabalina⁵⁶, N.W. Shaikh^{147a,147b}, L.Y. Shan^{35a},
 R. Shang¹⁶⁶, J.T. Shank²⁴, M. Shapiro¹⁶, P.B. Shatalov⁹⁸, K. Shaw^{164a,164b}, S.M. Shaw⁸⁶,
 A. Shcherbakova^{147a,147b}, C.Y. Shehu¹⁵⁰, P. Sherwood⁸⁰, L. Shi^{152,ai}, S. Shimizu⁶⁹, C.O. Shimmin¹⁶³,
 M. Shimojima¹⁰³, M. Shiyakova^{67,aj}, A. Shmeleva⁹⁷, D. Shoaleh Saadi⁹⁶, M.J. Shochet³³,

S. Shojaii^{93a,93b}, S. Shrestha¹¹², E. Shulga⁹⁹, M.A. Shupe⁷, P. Sicho¹²⁸, A.M. Sickles¹⁶⁶, P.E. Sidebo¹⁴⁸, O. Sidiropoulou¹⁷⁴, D. Sidorov¹¹⁵, A. Sidoti^{22a,22b}, F. Siegert⁴⁶, Dj. Sijacki¹⁴, J. Silva^{127a,127d}, S.B. Silverstein^{147a}, V. Simak¹²⁹, O. Simard⁵, Lj. Simic¹⁴, S. Simion¹¹⁸, E. Simioni⁸⁵, B. Simmons⁸⁰, D. Simon³⁶, M. Simon⁸⁵, P. Sinervo¹⁵⁹, N.B. Sinev¹¹⁷, M. Sioli^{22a,22b}, G. Siragusa¹⁷⁴, S.Yu. Sivoklokov¹⁰⁰, J. Sjölin^{147a,147b}, T.B. Sjursen¹⁵, M.B. Skinner⁷⁴, H.P. Skottowe⁵⁹, P. Skubic¹¹⁴, M. Slater¹⁹, T. Slavicek¹²⁹, M. Slawinska¹⁰⁸, K. Sliwa¹⁶², R. Slovak¹³⁰, V. Smakhtin¹⁷², B.H. Smart⁵, L. Smestad¹⁵, J. Smiesko^{145a}, S.Yu. Smirnov⁹⁹, Y. Smirnov⁹⁹, L.N. Smirnova^{100,ak}, O. Smirnova⁸³, M.N.K. Smith³⁷, R.W. Smith³⁷, M. Smizanska⁷⁴, K. Smolek¹²⁹, A.A. Snesarev⁹⁷, S. Snyder²⁷, R. Sobie^{169,l}, F. Socher⁴⁶, A. Soffer¹⁵⁴, D.A. Soh¹⁵², G. Sokhrannyi⁷⁷, C.A. Solans Sanchez³², M. Solar¹²⁹, E.Yu. Soldatov⁹⁹, U. Soldevila¹⁶⁷, A.A. Solodkov¹³¹, A. Soloshenko⁶⁷, O.V. Solovyanov¹³¹, V. Solovyev¹²⁴, P. Sommer⁵⁰, H. Son¹⁶², H.Y. Song^{35b,aa}, A. Sood¹⁶, A. Sopczak¹²⁹, V. Sopko¹²⁹, V. Sorin¹³, D. Sosa^{60b}, C.L. Sotiropoulou^{125a,125b}, R. Soualah^{164a,164c}, A.M. Soukharev^{110,c}, D. South⁴⁴, B.C. Sowden⁷⁹, S. Spagnolo^{75a,75b}, M. Spalla^{125a,125b}, M. Spangenberg¹⁷⁰, F. Spanò⁷⁹, D. Sperlich¹⁷, F. Spettel¹⁰², R. Spighi^{22a}, G. Spigo³², L.A. Spiller⁹⁰, M. Spousta¹³⁰, R.D. St. Denis^{55,*}, A. Stabile^{93a}, R. Stamen^{60a}, S. Stamm¹⁷, E. Stanecka⁴¹, R.W. Stanek⁶, C. Stanescu^{135a}, M. Stanescu-Bellu⁴⁴, M.M. Stanitzki⁴⁴, S. Stapnes¹²⁰, E.A. Starchenko¹³¹, G.H. Stark³³, J. Stark⁵⁷, P. Staroba¹²⁸, P. Starovoitov^{60a}, S. Stärz³², R. Staszewski⁴¹, P. Steinberg²⁷, B. Stelzer¹⁴³, H.J. Stelzer³², O. Stelzer-Chilton^{160a}, H. Stenzel⁵⁴, G.A. Stewart⁵⁵, J.A. Stillings²³, M.C. Stockton⁸⁹, M. Stoebe⁸⁹, G. Stoica^{28b}, P. Stolte⁵⁶, S. Stonjek¹⁰², A.R. Stradling⁸, A. Straessner⁴⁶, M.E. Stramaglia¹⁸, J. Strandberg¹⁴⁸, S. Strandberg^{147a,147b}, A. Strandlie¹²⁰, M. Strauss¹¹⁴, P. Strizenec^{145b}, R. Ströhmer¹⁷⁴, D.M. Strom¹¹⁷, R. Stroynowski⁴², A. Strubig¹⁰⁷, S.A. Stucci¹⁸, B. Stugu¹⁵, N.A. Styles⁴⁴, D. Su¹⁴⁴, J. Su¹²⁶, R. Subramaniam⁸¹, S. Suchek^{60a}, Y. Sugaya¹¹⁹, M. Suk¹²⁹, V.V. Sulin⁹⁷, S. Sultansoy^{4c}, T. Sumida⁷⁰, S. Sun⁵⁹, X. Sun^{35a}, J.E. Sundermann⁵⁰, K. Suruliz¹⁵⁰, G. Susinno^{39a,39b}, M.R. Sutton¹⁵⁰, S. Suzuki⁶⁸, M. Svatos¹²⁸, M. Swiatlowski³³, I. Sykora^{145a}, T. Sykora¹³⁰, D. Ta⁵⁰, C. Taccini^{135a,135b}, K. Tackmann⁴⁴, J. Taenzer¹⁵⁹, A. Taffard¹⁶³, R. Tafirout^{160a}, N. Taiblum¹⁵⁴, H. Takai²⁷, R. Takashima⁷¹, T. Takeshita¹⁴¹, Y. Takubo⁶⁸, M. Talby⁸⁷, A.A. Talyshev^{110,c}, K.G. Tan⁹⁰, J. Tanaka¹⁵⁶, R. Tanaka¹¹⁸, S. Tanaka⁶⁸, B.B. Tannenwald¹¹², S. Tapia Araya^{34b}, S. Tapprogge⁸⁵, S. Tarem¹⁵³, G.F. Tartarelli^{93a}, P. Tas¹³⁰, M. Tasevsky¹²⁸, T. Tashiro⁷⁰, E. Tassi^{39a,39b}, A. Tavares Delgado^{127a,127b}, Y. Tayalati^{136d}, A.C. Taylor¹⁰⁶, G.N. Taylor⁹⁰, P.T.E. Taylor⁹⁰, W. Taylor^{160b}, F.A. Teischinger³², P. Teixeira-Dias⁷⁹, K.K. Temming⁵⁰, D. Temple¹⁴³, H. Ten Kate³², P.K. Teng¹⁵², J.J. Teoh¹¹⁹, F. Tepel¹⁷⁵, S. Terada⁶⁸, K. Terashi¹⁵⁶, J. Terron⁸⁴, S. Terzo¹⁰², M. Testa⁴⁹, R.J. Teuscher^{159,l}, T. Theveneaux-Pelzer⁸⁷, J.P. Thomas¹⁹, J. Thomas-Wilsker⁷⁹, E.N. Thompson³⁷, P.D. Thompson¹⁹, A.S. Thompson⁵⁵, L.A. Thomsen¹⁷⁶, E. Thomson¹²³, M. Thomson³⁰, M.J. Tibbetts¹⁶, R.E. Ticse Torres⁸⁷, V.O. Tikhomirov^{97,al}, Yu.A. Tikhonov^{110,c}, S. Timoshenko⁹⁹, P. Tipton¹⁷⁶, S. Tisserant⁸⁷, K. Todome¹⁵⁸, T. Todorov^{5,*}, S. Todorova-Nova¹³⁰, J. Tojo⁷², S. Tokár^{145a}, K. Tokushuku⁶⁸, E. Tolley⁵⁹, L. Tomlinson⁸⁶, M. Tomoto¹⁰⁴, L. Tompkins^{144,am}, K. Toms¹⁰⁶, B. Tong⁵⁹, E. Torrence¹¹⁷, H. Torres¹⁴³, E. Torró Pastor¹³⁹, J. Toth^{87,an}, F. Touchard⁸⁷, D.R. Tovey¹⁴⁰, T. Trefzger¹⁷⁴, A. Tricoli²⁷, I.M. Trigger^{160a}, S. Trincaz-Duvold⁸², M.F. Tripiana¹³, W. Trischuk¹⁵⁹, B. Trocmé⁵⁷, A. Trofymov⁴⁴, C. Troncon^{93a}, M. Trottier-McDonald¹⁶, M. Trovatelli¹⁶⁹, L. Truong^{164a,164c}, M. Trzebinski⁴¹, A. Trzupek⁴¹, J.C-L. Tseng¹²¹, P.V. Tsiareshka⁹⁴, G. Tsipolitis¹⁰, N. Tsirintanis⁹, S. Tsiskaridze¹³, V. Tsiskaridze⁵⁰, E.G. Tskhadadze^{53a}, K.M. Tsui^{62a}, I.I. Tsukerman⁹⁸, V. Tsulaia¹⁶, S. Tsuno⁶⁸, D. Tsybychev¹⁴⁹, A. Tudorache^{28b}, V. Tudorache^{28b}, A.N. Tuna⁵⁹, S.A. Tupputi^{22a,22b}, S. Turchikhin^{100,ak}, D. Turecek¹²⁹, D. Turgeman¹⁷², R. Turra^{93a,93b}, A.J. Turvey⁴², P.M. Tuts³⁷, M. Tyndel¹³², G. Ucchielli^{22a,22b}, I. Ueda¹⁵⁶, R. Ueno³¹, M. Ughetto^{147a,147b}, F. Ukegawa¹⁶¹, G. Unal³², A. Undrus²⁷, G. Unel¹⁶³, F.C. Ungaro⁹⁰, Y. Unno⁶⁸, C. Unverdorben¹⁰¹, J. Urban^{145b}, P. Urquijo⁹⁰, P. Urrejola⁸⁵, G. Usai⁸, A. Usanova⁶⁴, L. Vacavant⁸⁷, V. Vacek¹²⁹, B. Vachon⁸⁹, C. Valderanis¹⁰¹, E. Valdes Santurio^{147a,147b}, N. Valencic¹⁰⁸, S. Valentinetto^{22a,22b},

A. Valero¹⁶⁷, L. Valery¹³, S. Valkar¹³⁰, S. Vallecorsa⁵¹, J.A. Valls Ferrer¹⁶⁷, W. Van Den Wollenberg¹⁰⁸, P.C. Van Der Deijl¹⁰⁸, R. van der Geer¹⁰⁸, H. van der Graaf¹⁰⁸, N. van Eldik¹⁵³, P. van Gemmeren⁶, J. Van Nieuwkoop¹⁴³, I. van Vulpen¹⁰⁸, M.C. van Woerden³², M. Vanadia^{133a,133b}, W. Vandelli³², R. Vanguri¹²³, A. Vaniachine¹³¹, P. Vankov¹⁰⁸, G. Vardanyan¹⁷⁷, R. Vari^{133a}, E.W. Varnes⁷, T. Varol⁴², D. Varouchas⁸², A. Vartapetian⁸, K.E. Varvell¹⁵¹, J.G. Vasquez¹⁷⁶, F. Vazeille³⁶, T. Vazquez Schroeder⁸⁹, J. Veatch⁵⁶, L.M. Veloce¹⁵⁹, F. Veloso^{127a,127c}, S. Veneziano^{133a}, A. Ventura^{75a,75b}, M. Venturi¹⁶⁹, N. Venturi¹⁵⁹, A. Venturini²⁵, V. Vercesi^{122a}, M. Verducci^{133a,133b}, W. Verkerke¹⁰⁸, J.C. Vermeulen¹⁰⁸, A. Vest^{46,ao}, M.C. Vetterli^{143,d}, O. Viazlo⁸³, I. Vichou¹⁶⁶, T. Vickey¹⁴⁰, O.E. Vickey Boeriu¹⁴⁰, G.H.A. Viehhauser¹²¹, S. Viel¹⁶, L. Vigani¹²¹, R. Vigne⁶⁴, M. Villa^{22a,22b}, M. Villaplana Perez^{93a,93b}, E. Vilucchi⁴⁹, M.G. Vincter³¹, V.B. Vinogradov⁶⁷, C. Vittori^{22a,22b}, I. Vivarelli¹⁵⁰, S. Vlachos¹⁰, M. Vlasak¹²⁹, M. Vogel¹⁷⁵, P. Vokac¹²⁹, G. Volpi^{125a,125b}, M. Volpi⁹⁰, H. von der Schmitt¹⁰², E. von Toerne²³, V. Vorobel¹³⁰, K. Vorobev⁹⁹, M. Vos¹⁶⁷, R. Voss³², J.H. Vossebeld⁷⁶, N. Vranjes¹⁴, M. Vranjes Milosavljevic¹⁴, V. Vrba¹²⁸, M. Vreeswijk¹⁰⁸, R. Vuillermet³², I. Vukotic³³, Z. Vykydal¹²⁹, P. Wagner²³, W. Wagner¹⁷⁵, H. Wahlberg⁷³, S. Wahrmund⁴⁶, J. Wakabayashi¹⁰⁴, J. Walder⁷⁴, R. Walker¹⁰¹, W. Walkowiak¹⁴², V. Wallangen^{147a,147b}, C. Wang^{35c}, C. Wang^{35d,87}, F. Wang¹⁷³, H. Wang¹⁶, H. Wang⁴², J. Wang⁴⁴, J. Wang¹⁵¹, K. Wang⁸⁹, R. Wang⁶, S.M. Wang¹⁵², T. Wang²³, T. Wang³⁷, W. Wang^{35b}, X. Wang¹⁷⁶, C. Wanotayaroj¹¹⁷, A. Warburton⁸⁹, C.P. Ward³⁰, D.R. Wardrop⁸⁰, A. Washbrook⁴⁸, P.M. Watkins¹⁹, A.T. Watson¹⁹, M.F. Watson¹⁹, G. Watts¹³⁹, S. Watts⁸⁶, B.M. Waugh⁸⁰, S. Webb⁸⁵, M.S. Weber¹⁸, S.W. Weber¹⁷⁴, J.S. Webster⁶, A.R. Weidberg¹²¹, B. Weinert⁶³, J. Weingarten⁵⁶, C. Weiser⁵⁰, H. Weits¹⁰⁸, P.S. Wells³², T. Wenaus²⁷, T. Wengler³², S. Wenig³², N. Wermes²³, M. Werner⁵⁰, P. Werner³², M. Wessels^{60a}, J. Wetter¹⁶², K. Whalen¹¹⁷, N.L. Whallon¹³⁹, A.M. Wharton⁷⁴, A. White⁸, M.J. White¹, R. White^{34b}, D. Whiteson¹⁶³, F.J. Wickens¹³², W. Wiedenmann¹⁷³, M. Wielers¹³², P. Wienemann²³, C. Wiglesworth³⁸, L.A.M. Wiik-Fuchs²³, A. Wildauer¹⁰², F. Wilk⁸⁶, H.G. Wilkens³², H.H. Williams¹²³, S. Williams¹⁰⁸, C. Willis⁹², S. Willocq⁸⁸, J.A. Wilson¹⁹, I. Wingerter-Seez⁵, F. Winklmeier¹¹⁷, O.J. Winston¹⁵⁰, B.T. Winter²³, M. Wittgen¹⁴⁴, J. Wittkowski¹⁰¹, S.J. Wollstadt⁸⁵, M.W. Wolter⁴¹, H. Wolters^{127a,127c}, B.K. Wosiek⁴¹, J. Wotschack³², M.J. Woudstra⁸⁶, K.W. Wozniak⁴¹, M. Wu⁵⁷, M. Wu³³, S.L. Wu¹⁷³, X. Wu⁵¹, Y. Wu⁹¹, T.R. Wyatt⁸⁶, B.M. Wynne⁴⁸, S. Xella³⁸, D. Xu^{35a}, L. Xu²⁷, B. Yabsley¹⁵¹, S. Yacoob^{146a}, R. Yakabe⁶⁹, D. Yamaguchi¹⁵⁸, Y. Yamaguchi¹¹⁹, A. Yamamoto⁶⁸, S. Yamamoto¹⁵⁶, T. Yamanaka¹⁵⁶, K. Yamauchi¹⁰⁴, Y. Yamazaki⁶⁹, Z. Yan²⁴, H. Yang^{35e}, H. Yang¹⁷³, Y. Yang¹⁵², Z. Yang¹⁵, W-M. Yao¹⁶, Y.C. Yap⁸², Y. Yasu⁶⁸, E. Yatsenko⁵, K.H. Yau Wong²³, J. Ye⁴², S. Ye²⁷, I. Yeletskikh⁶⁷, A.L. Yen⁵⁹, E. Yildirim⁸⁵, K. Yorita¹⁷¹, R. Yoshida⁶, K. Yoshihara¹²³, C. Young¹⁴⁴, C.J.S. Young³², S. Youssef²⁴, D.R. Yu¹⁶, J. Yu⁸, J.M. Yu⁹¹, J. Yu⁶⁶, L. Yuan⁶⁹, S.P.Y. Yuen²³, I. Yusuff^{30,ap}, B. Zabinski⁴¹, R. Zaidan^{35d}, A.M. Zaitsev^{131,ad}, N. Zakharchuk⁴⁴, J. Zalieckas¹⁵, A. Zaman¹⁴⁹, S. Zambito⁵⁹, L. Zanello^{133a,133b}, D. Zanzi⁹⁰, C. Zeitnitz¹⁷⁵, M. Zeman¹²⁹, A. Zemla^{40a}, J.C. Zeng¹⁶⁶, Q. Zeng¹⁴⁴, K. Zengel²⁵, O. Zenin¹³¹, T. Ženiš^{145a}, D. Zerwas¹¹⁸, D. Zhang⁹¹, F. Zhang¹⁷³, G. Zhang^{35b,aa}, H. Zhang^{35c}, J. Zhang⁶, L. Zhang⁵⁰, R. Zhang²³, R. Zhang^{35b,aq}, X. Zhang^{35d}, Z. Zhang¹¹⁸, X. Zhao⁴², Y. Zhao^{35d,118}, Z. Zhao^{35b}, A. Zhemchugov⁶⁷, J. Zhong¹²¹, B. Zhou⁹¹, C. Zhou⁴⁷, L. Zhou³⁷, L. Zhou⁴², M. Zhou¹⁴⁹, N. Zhou^{35f}, C.G. Zhu^{35d}, H. Zhu^{35a}, J. Zhu⁹¹, Y. Zhu^{35b}, X. Zhuang^{35a}, K. Zhukov⁹⁷, A. Zibell¹⁷⁴, D. Ziemińska⁶³, N.I. Zimine⁶⁷, C. Zimmermann⁸⁵, S. Zimmermann⁵⁰, Z. Zinonos⁵⁶, M. Zinser⁸⁵, M. Ziolkowski¹⁴², L. Živković¹⁴, G. Zobernig¹⁷³, A. Zoccoli^{22a,22b}, M. zur Nedden¹⁷, G. Zurzolo^{105a,105b}, L. Zwalski³².

¹ Department of Physics, University of Adelaide, Adelaide, Australia

² Physics Department, SUNY Albany, Albany NY, United States of America

³ Department of Physics, University of Alberta, Edmonton AB, Canada

⁴ ^(a) Department of Physics, Ankara University, Ankara; ^(b) Istanbul Aydin University, Istanbul; ^(c)

- Division of Physics, TOBB University of Economics and Technology, Ankara, Turkey
- ⁵ LAPP, CNRS/IN2P3 and Université Savoie Mont Blanc, Annecy-le-Vieux, France
- ⁶ High Energy Physics Division, Argonne National Laboratory, Argonne IL, United States of America
- ⁷ Department of Physics, University of Arizona, Tucson AZ, United States of America
- ⁸ Department of Physics, The University of Texas at Arlington, Arlington TX, United States of America
- ⁹ Physics Department, University of Athens, Athens, Greece
- ¹⁰ Physics Department, National Technical University of Athens, Zografou, Greece
- ¹¹ Department of Physics, The University of Texas at Austin, Austin TX, United States of America
- ¹² Institute of Physics, Azerbaijan Academy of Sciences, Baku, Azerbaijan
- ¹³ Institut de Física d'Altes Energies (IFAE), The Barcelona Institute of Science and Technology, Barcelona, Spain, Spain
- ¹⁴ Institute of Physics, University of Belgrade, Belgrade, Serbia
- ¹⁵ Department for Physics and Technology, University of Bergen, Bergen, Norway
- ¹⁶ Physics Division, Lawrence Berkeley National Laboratory and University of California, Berkeley CA, United States of America
- ¹⁷ Department of Physics, Humboldt University, Berlin, Germany
- ¹⁸ Albert Einstein Center for Fundamental Physics and Laboratory for High Energy Physics, University of Bern, Bern, Switzerland
- ¹⁹ School of Physics and Astronomy, University of Birmingham, Birmingham, United Kingdom
- ²⁰ ^(a) Department of Physics, Bogazici University, Istanbul; ^(b) Department of Physics Engineering, Gaziantep University, Gaziantep; ^(d) Istanbul Bilgi University, Faculty of Engineering and Natural Sciences, Istanbul, Turkey; ^(e) Bahcesehir University, Faculty of Engineering and Natural Sciences, Istanbul, Turkey, Turkey
- ²¹ Centro de Investigaciones, Universidad Antonio Narino, Bogota, Colombia
- ²² ^(a) INFN Sezione di Bologna; ^(b) Dipartimento di Fisica e Astronomia, Università di Bologna, Bologna, Italy
- ²³ Physikalisches Institut, University of Bonn, Bonn, Germany
- ²⁴ Department of Physics, Boston University, Boston MA, United States of America
- ²⁵ Department of Physics, Brandeis University, Waltham MA, United States of America
- ²⁶ ^(a) Universidade Federal do Rio De Janeiro COPPE/EE/IF, Rio de Janeiro; ^(b) Electrical Circuits Department, Federal University of Juiz de Fora (UFJF), Juiz de Fora; ^(c) Federal University of Sao Joao del Rei (UFSJ), Sao Joao del Rei; ^(d) Instituto de Fisica, Universidade de Sao Paulo, Sao Paulo, Brazil
- ²⁷ Physics Department, Brookhaven National Laboratory, Upton NY, United States of America
- ²⁸ ^(a) Transilvania University of Brasov, Brasov, Romania; ^(b) National Institute of Physics and Nuclear Engineering, Bucharest; ^(c) National Institute for Research and Development of Isotopic and Molecular Technologies, Physics Department, Cluj Napoca; ^(d) University Politehnica Bucharest, Bucharest; ^(e) West University in Timisoara, Timisoara, Romania
- ²⁹ Departamento de Física, Universidad de Buenos Aires, Buenos Aires, Argentina
- ³⁰ Cavendish Laboratory, University of Cambridge, Cambridge, United Kingdom
- ³¹ Department of Physics, Carleton University, Ottawa ON, Canada
- ³² CERN, Geneva, Switzerland
- ³³ Enrico Fermi Institute, University of Chicago, Chicago IL, United States of America
- ³⁴ ^(a) Departamento de Física, Pontificia Universidad Católica de Chile, Santiago; ^(b) Departamento de Física, Universidad Técnica Federico Santa María, Valparaíso, Chile
- ³⁵ ^(a) Institute of High Energy Physics, Chinese Academy of Sciences, Beijing; ^(b) Department of Modern Physics, University of Science and Technology of China, Anhui; ^(c) Department of Physics, Nanjing University, Jiangsu; ^(d) School of Physics, Shandong University, Shandong; ^(e) Department of

Physics and Astronomy, Shanghai Key Laboratory for Particle Physics and Cosmology, Shanghai Jiao Tong University, Shanghai; (also affiliated with PKU-CHEP); ^(f) Physics Department, Tsinghua University, Beijing 100084, China

³⁶ Laboratoire de Physique Corpusculaire, Clermont Université and Université Blaise Pascal and CNRS/IN2P3, Clermont-Ferrand, France

³⁷ Nevis Laboratory, Columbia University, Irvington NY, United States of America

³⁸ Niels Bohr Institute, University of Copenhagen, Kobenhavn, Denmark

³⁹ ^(a) INFN Gruppo Collegato di Cosenza, Laboratori Nazionali di Frascati; ^(b) Dipartimento di Fisica, Università della Calabria, Rende, Italy

⁴⁰ ^(a) AGH University of Science and Technology, Faculty of Physics and Applied Computer Science, Krakow; ^(b) Marian Smoluchowski Institute of Physics, Jagiellonian University, Krakow, Poland

⁴¹ Institute of Nuclear Physics Polish Academy of Sciences, Krakow, Poland

⁴² Physics Department, Southern Methodist University, Dallas TX, United States of America

⁴³ Physics Department, University of Texas at Dallas, Richardson TX, United States of America

⁴⁴ DESY, Hamburg and Zeuthen, Germany

⁴⁵ Institut für Experimentelle Physik IV, Technische Universität Dortmund, Dortmund, Germany

⁴⁶ Institut für Kern- und Teilchenphysik, Technische Universität Dresden, Dresden, Germany

⁴⁷ Department of Physics, Duke University, Durham NC, United States of America

⁴⁸ SUPA - School of Physics and Astronomy, University of Edinburgh, Edinburgh, United Kingdom

⁴⁹ INFN Laboratori Nazionali di Frascati, Frascati, Italy

⁵⁰ Fakultät für Mathematik und Physik, Albert-Ludwigs-Universität, Freiburg, Germany

⁵¹ Section de Physique, Université de Genève, Geneva, Switzerland

⁵² ^(a) INFN Sezione di Genova; ^(b) Dipartimento di Fisica, Università di Genova, Genova, Italy

⁵³ ^(a) E. Andronikashvili Institute of Physics, Iv. Javakhishvili Tbilisi State University, Tbilisi; ^(b) High Energy Physics Institute, Tbilisi State University, Tbilisi, Georgia

⁵⁴ II Physikalisches Institut, Justus-Liebig-Universität Giessen, Giessen, Germany

⁵⁵ SUPA - School of Physics and Astronomy, University of Glasgow, Glasgow, United Kingdom

⁵⁶ II Physikalisches Institut, Georg-August-Universität, Göttingen, Germany

⁵⁷ Laboratoire de Physique Subatomique et de Cosmologie, Université Grenoble-Alpes, CNRS/IN2P3, Grenoble, France

⁵⁸ Department of Physics, Hampton University, Hampton VA, United States of America

⁵⁹ Laboratory for Particle Physics and Cosmology, Harvard University, Cambridge MA, United States of America

⁶⁰ ^(a) Kirchhoff-Institut für Physik, Ruprecht-Karls-Universität Heidelberg, Heidelberg; ^(b) Physikalisches Institut, Ruprecht-Karls-Universität Heidelberg, Heidelberg; ^(c) ZITI Institut für technische Informatik, Ruprecht-Karls-Universität Heidelberg, Mannheim, Germany

⁶¹ Faculty of Applied Information Science, Hiroshima Institute of Technology, Hiroshima, Japan

⁶² ^(a) Department of Physics, The Chinese University of Hong Kong, Shatin, N.T., Hong Kong; ^(b) Department of Physics, The University of Hong Kong, Hong Kong; ^(c) Department of Physics, The Hong Kong University of Science and Technology, Clear Water Bay, Kowloon, Hong Kong, China

⁶³ Department of Physics, Indiana University, Bloomington IN, United States of America

⁶⁴ Institut für Astro- und Teilchenphysik, Leopold-Franzens-Universität, Innsbruck, Austria

⁶⁵ University of Iowa, Iowa City IA, United States of America

⁶⁶ Department of Physics and Astronomy, Iowa State University, Ames IA, United States of America

⁶⁷ Joint Institute for Nuclear Research, JINR Dubna, Dubna, Russia

⁶⁸ KEK, High Energy Accelerator Research Organization, Tsukuba, Japan

⁶⁹ Graduate School of Science, Kobe University, Kobe, Japan

- ⁷⁰ Faculty of Science, Kyoto University, Kyoto, Japan
⁷¹ Kyoto University of Education, Kyoto, Japan
⁷² Department of Physics, Kyushu University, Fukuoka, Japan
⁷³ Instituto de Física La Plata, Universidad Nacional de La Plata and CONICET, La Plata, Argentina
⁷⁴ Physics Department, Lancaster University, Lancaster, United Kingdom
⁷⁵ ^(a) INFN Sezione di Lecce; ^(b) Dipartimento di Matematica e Fisica, Università del Salento, Lecce, Italy
⁷⁶ Oliver Lodge Laboratory, University of Liverpool, Liverpool, United Kingdom
⁷⁷ Department of Physics, Jožef Stefan Institute and University of Ljubljana, Ljubljana, Slovenia
⁷⁸ School of Physics and Astronomy, Queen Mary University of London, London, United Kingdom
⁷⁹ Department of Physics, Royal Holloway University of London, Surrey, United Kingdom
⁸⁰ Department of Physics and Astronomy, University College London, London, United Kingdom
⁸¹ Louisiana Tech University, Ruston LA, United States of America
⁸² Laboratoire de Physique Nucléaire et de Hautes Energies, UPMC and Université Paris-Diderot and CNRS/IN2P3, Paris, France
⁸³ Fysiska institutionen, Lunds universitet, Lund, Sweden
⁸⁴ Departamento de Fisica Teorica C-15, Universidad Autonoma de Madrid, Madrid, Spain
⁸⁵ Institut für Physik, Universität Mainz, Mainz, Germany
⁸⁶ School of Physics and Astronomy, University of Manchester, Manchester, United Kingdom
⁸⁷ CPPM, Aix-Marseille Université and CNRS/IN2P3, Marseille, France
⁸⁸ Department of Physics, University of Massachusetts, Amherst MA, United States of America
⁸⁹ Department of Physics, McGill University, Montreal QC, Canada
⁹⁰ School of Physics, University of Melbourne, Victoria, Australia
⁹¹ Department of Physics, The University of Michigan, Ann Arbor MI, United States of America
⁹² Department of Physics and Astronomy, Michigan State University, East Lansing MI, United States of America
⁹³ ^(a) INFN Sezione di Milano; ^(b) Dipartimento di Fisica, Università di Milano, Milano, Italy
⁹⁴ B.I. Stepanov Institute of Physics, National Academy of Sciences of Belarus, Minsk, Republic of Belarus
⁹⁵ National Scientific and Educational Centre for Particle and High Energy Physics, Minsk, Republic of Belarus
⁹⁶ Group of Particle Physics, University of Montreal, Montreal QC, Canada
⁹⁷ P.N. Lebedev Physical Institute of the Russian Academy of Sciences, Moscow, Russia
⁹⁸ Institute for Theoretical and Experimental Physics (ITEP), Moscow, Russia
⁹⁹ National Research Nuclear University MEPhI, Moscow, Russia
¹⁰⁰ D.V. Skobeltsyn Institute of Nuclear Physics, M.V. Lomonosov Moscow State University, Moscow, Russia
¹⁰¹ Fakultät für Physik, Ludwig-Maximilians-Universität München, München, Germany
¹⁰² Max-Planck-Institut für Physik (Werner-Heisenberg-Institut), München, Germany
¹⁰³ Nagasaki Institute of Applied Science, Nagasaki, Japan
¹⁰⁴ Graduate School of Science and Kobayashi-Maskawa Institute, Nagoya University, Nagoya, Japan
¹⁰⁵ ^(a) INFN Sezione di Napoli; ^(b) Dipartimento di Fisica, Università di Napoli, Napoli, Italy
¹⁰⁶ Department of Physics and Astronomy, University of New Mexico, Albuquerque NM, United States of America
¹⁰⁷ Institute for Mathematics, Astrophysics and Particle Physics, Radboud University Nijmegen/Nikhef, Nijmegen, Netherlands
¹⁰⁸ Nikhef National Institute for Subatomic Physics and University of Amsterdam, Amsterdam,

Netherlands

¹⁰⁹ Department of Physics, Northern Illinois University, DeKalb IL, United States of America

¹¹⁰ Budker Institute of Nuclear Physics, SB RAS, Novosibirsk, Russia

¹¹¹ Department of Physics, New York University, New York NY, United States of America

¹¹² Ohio State University, Columbus OH, United States of America

¹¹³ Faculty of Science, Okayama University, Okayama, Japan

¹¹⁴ Homer L. Dodge Department of Physics and Astronomy, University of Oklahoma, Norman OK, United States of America

¹¹⁵ Department of Physics, Oklahoma State University, Stillwater OK, United States of America

¹¹⁶ Palacký University, RCPTM, Olomouc, Czech Republic

¹¹⁷ Center for High Energy Physics, University of Oregon, Eugene OR, United States of America

¹¹⁸ LAL, Univ. Paris-Sud, CNRS/IN2P3, Université Paris-Saclay, Orsay, France

¹¹⁹ Graduate School of Science, Osaka University, Osaka, Japan

¹²⁰ Department of Physics, University of Oslo, Oslo, Norway

¹²¹ Department of Physics, Oxford University, Oxford, United Kingdom

¹²² ^(a) INFN Sezione di Pavia; ^(b) Dipartimento di Fisica, Università di Pavia, Pavia, Italy

¹²³ Department of Physics, University of Pennsylvania, Philadelphia PA, United States of America

¹²⁴ National Research Centre "Kurchatov Institute" B.P.Konstantinov Petersburg Nuclear Physics Institute, St. Petersburg, Russia

¹²⁵ ^(a) INFN Sezione di Pisa; ^(b) Dipartimento di Fisica E. Fermi, Università di Pisa, Pisa, Italy

¹²⁶ Department of Physics and Astronomy, University of Pittsburgh, Pittsburgh PA, United States of America

¹²⁷ ^(a) Laboratório de Instrumentação e Física Experimental de Partículas - LIP, Lisboa; ^(b) Faculdade de Ciências, Universidade de Lisboa, Lisboa; ^(c) Department of Physics, University of Coimbra, Coimbra; ^(d) Centro de Física Nuclear da Universidade de Lisboa, Lisboa; ^(e) Departamento de Física, Universidade do Minho, Braga; ^(f) Departamento de Física Teórica y del Cosmos and CAFPE, Universidad de Granada, Granada (Spain); ^(g) Dep Física and CEFITEC of Faculdade de Ciencias e Tecnologia, Universidade Nova de Lisboa, Caparica, Portugal

¹²⁸ Institute of Physics, Academy of Sciences of the Czech Republic, Praha, Czech Republic

¹²⁹ Czech Technical University in Prague, Praha, Czech Republic

¹³⁰ Faculty of Mathematics and Physics, Charles University in Prague, Praha, Czech Republic

¹³¹ State Research Center Institute for High Energy Physics (Protvino), NRC KI, Russia

¹³² Particle Physics Department, Rutherford Appleton Laboratory, Didcot, United Kingdom

¹³³ ^(a) INFN Sezione di Roma; ^(b) Dipartimento di Fisica, Sapienza Università di Roma, Roma, Italy

¹³⁴ ^(a) INFN Sezione di Roma Tor Vergata; ^(b) Dipartimento di Fisica, Università di Roma Tor Vergata, Roma, Italy

¹³⁵ ^(a) INFN Sezione di Roma Tre; ^(b) Dipartimento di Matematica e Fisica, Università Roma Tre, Roma, Italy

¹³⁶ ^(a) Faculté des Sciences Ain Chock, Réseau Universitaire de Physique des Hautes Energies - Université Hassan II, Casablanca; ^(b) Centre National de l'Energie des Sciences Techniques Nucléaires, Rabat; ^(c) Faculté des Sciences Semlalia, Université Cadi Ayyad, LPHEA-Marrakech; ^(d) Faculté des Sciences, Université Mohamed Premier and LPTPM, Oujda; ^(e) Faculté des sciences, Université Mohammed V, Rabat, Morocco

¹³⁷ DSM/IRFU (Institut de Recherches sur les Lois Fondamentales de l'Univers), CEA Saclay (Commissariat à l'Energie Atomique et aux Energies Alternatives), Gif-sur-Yvette, France

¹³⁸ Santa Cruz Institute for Particle Physics, University of California Santa Cruz, Santa Cruz CA, United States of America

- ¹³⁹ Department of Physics, University of Washington, Seattle WA, United States of America
¹⁴⁰ Department of Physics and Astronomy, University of Sheffield, Sheffield, United Kingdom
¹⁴¹ Department of Physics, Shinshu University, Nagano, Japan
¹⁴² Fachbereich Physik, Universität Siegen, Siegen, Germany
¹⁴³ Department of Physics, Simon Fraser University, Burnaby BC, Canada
¹⁴⁴ SLAC National Accelerator Laboratory, Stanford CA, United States of America
¹⁴⁵ ^(a) Faculty of Mathematics, Physics & Informatics, Comenius University, Bratislava; ^(b) Department of Subnuclear Physics, Institute of Experimental Physics of the Slovak Academy of Sciences, Kosice, Slovak Republic
¹⁴⁶ ^(a) Department of Physics, University of Cape Town, Cape Town; ^(b) Department of Physics, University of Johannesburg, Johannesburg; ^(c) School of Physics, University of the Witwatersrand, Johannesburg, South Africa
¹⁴⁷ ^(a) Department of Physics, Stockholm University; ^(b) The Oskar Klein Centre, Stockholm, Sweden
¹⁴⁸ Physics Department, Royal Institute of Technology, Stockholm, Sweden
¹⁴⁹ Departments of Physics & Astronomy and Chemistry, Stony Brook University, Stony Brook NY, United States of America
¹⁵⁰ Department of Physics and Astronomy, University of Sussex, Brighton, United Kingdom
¹⁵¹ School of Physics, University of Sydney, Sydney, Australia
¹⁵² Institute of Physics, Academia Sinica, Taipei, Taiwan
¹⁵³ Department of Physics, Technion: Israel Institute of Technology, Haifa, Israel
¹⁵⁴ Raymond and Beverly Sackler School of Physics and Astronomy, Tel Aviv University, Tel Aviv, Israel
¹⁵⁵ Department of Physics, Aristotle University of Thessaloniki, Thessaloniki, Greece
¹⁵⁶ International Center for Elementary Particle Physics and Department of Physics, The University of Tokyo, Tokyo, Japan
¹⁵⁷ Graduate School of Science and Technology, Tokyo Metropolitan University, Tokyo, Japan
¹⁵⁸ Department of Physics, Tokyo Institute of Technology, Tokyo, Japan
¹⁵⁹ Department of Physics, University of Toronto, Toronto ON, Canada
¹⁶⁰ ^(a) TRIUMF, Vancouver BC; ^(b) Department of Physics and Astronomy, York University, Toronto ON, Canada
¹⁶¹ Faculty of Pure and Applied Sciences, and Center for Integrated Research in Fundamental Science and Engineering, University of Tsukuba, Tsukuba, Japan
¹⁶² Department of Physics and Astronomy, Tufts University, Medford MA, United States of America
¹⁶³ Department of Physics and Astronomy, University of California Irvine, Irvine CA, United States of America
¹⁶⁴ ^(a) INFN Gruppo Collegato di Udine, Sezione di Trieste, Udine; ^(b) ICTP, Trieste; ^(c) Dipartimento di Chimica, Fisica e Ambiente, Università di Udine, Udine, Italy
¹⁶⁵ Department of Physics and Astronomy, University of Uppsala, Uppsala, Sweden
¹⁶⁶ Department of Physics, University of Illinois, Urbana IL, United States of America
¹⁶⁷ Instituto de Física Corpuscular (IFIC) and Departamento de Física Atomica, Molecular y Nuclear and Departamento de Ingeniería Electrónica and Instituto de Microelectrónica de Barcelona (IMB-CNM), University of Valencia and CSIC, Valencia, Spain
¹⁶⁸ Department of Physics, University of British Columbia, Vancouver BC, Canada
¹⁶⁹ Department of Physics and Astronomy, University of Victoria, Victoria BC, Canada
¹⁷⁰ Department of Physics, University of Warwick, Coventry, United Kingdom
¹⁷¹ Waseda University, Tokyo, Japan
¹⁷² Department of Particle Physics, The Weizmann Institute of Science, Rehovot, Israel

- ¹⁷³ Department of Physics, University of Wisconsin, Madison WI, United States of America
¹⁷⁴ Fakultät für Physik und Astronomie, Julius-Maximilians-Universität, Würzburg, Germany
¹⁷⁵ Fakultät für Mathematik und Naturwissenschaften, Fachgruppe Physik, Bergische Universität Wuppertal, Wuppertal, Germany
¹⁷⁶ Department of Physics, Yale University, New Haven CT, United States of America
¹⁷⁷ Yerevan Physics Institute, Yerevan, Armenia
¹⁷⁸ Centre de Calcul de l’Institut National de Physique Nucléaire et de Physique des Particules (IN2P3), Villeurbanne, France
^a Also at Department of Physics, King’s College London, London, United Kingdom
^b Also at Institute of Physics, Azerbaijan Academy of Sciences, Baku, Azerbaijan
^c Also at Novosibirsk State University, Novosibirsk, Russia
^d Also at TRIUMF, Vancouver BC, Canada
^e Also at Department of Physics & Astronomy, University of Louisville, Louisville, KY, United States of America
^f Also at Department of Physics, California State University, Fresno CA, United States of America
^g Also at Department of Physics, University of Fribourg, Fribourg, Switzerland
^h Also at Departament de Fisica de la Universitat Autonoma de Barcelona, Barcelona, Spain
ⁱ Also at Departamento de Fisica e Astronomia, Faculdade de Ciencias, Universidade do Porto, Portugal
^j Also at Tomsk State University, Tomsk, Russia
^k Also at Universita di Napoli Parthenope, Napoli, Italy
^l Also at Institute of Particle Physics (IPP), Canada
^m Also at National Institute of Physics and Nuclear Engineering, Bucharest, Romania
ⁿ Also at Department of Physics, St. Petersburg State Polytechnical University, St. Petersburg, Russia
^o Also at Department of Physics, The University of Michigan, Ann Arbor MI, United States of America
^p Also at Louisiana Tech University, Ruston LA, United States of America
^q Also at Institutio Catalana de Recerca i Estudis Avancats, ICREA, Barcelona, Spain
^r Also at Graduate School of Science, Osaka University, Osaka, Japan
^s Also at Department of Physics, National Tsing Hua University, Taiwan
^t Also at Department of Physics, The University of Texas at Austin, Austin TX, United States of America
^u Also at Institute of Theoretical Physics, Ilia State University, Tbilisi, Georgia
^v Also at CERN, Geneva, Switzerland
^w Also at Georgian Technical University (GTU),Tbilisi, Georgia
^x Also at Ochadai Academic Production, Ochanomizu University, Tokyo, Japan
^y Also at Manhattan College, New York NY, United States of America
^z Also at Hellenic Open University, Patras, Greece
^{aa} Also at Institute of Physics, Academia Sinica, Taipei, Taiwan
^{ab} Also at Academia Sinica Grid Computing, Institute of Physics, Academia Sinica, Taipei, Taiwan
^{ac} Also at School of Physics, Shandong University, Shandong, China
^{ad} Also at Moscow Institute of Physics and Technology State University, Dolgoprudny, Russia
^{ae} Also at Section de Physique, Université de Genève, Geneva, Switzerland
^{af} Also at Eotvos Lorand University, Budapest, Hungary
^{ag} Also at International School for Advanced Studies (SISSA), Trieste, Italy
^{ah} Also at Department of Physics and Astronomy, University of South Carolina, Columbia SC, United States of America
^{ai} Also at School of Physics and Engineering, Sun Yat-sen University, Guangzhou, China
^{aj} Also at Institute for Nuclear Research and Nuclear Energy (INRNE) of the Bulgarian Academy of Sciences, Sofia, Bulgaria

ak Also at Faculty of Physics, M.V.Lomonosov Moscow State University, Moscow, Russia

al Also at National Research Nuclear University MEPhI, Moscow, Russia

am Also at Department of Physics, Stanford University, Stanford CA, United States of America

an Also at Institute for Particle and Nuclear Physics, Wigner Research Centre for Physics, Budapest, Hungary

ao Also at Flensburg University of Applied Sciences, Flensburg, Germany

ap Also at University of Malaya, Department of Physics, Kuala Lumpur, Malaysia

aq Also at CPPM, Aix-Marseille Université and CNRS/IN2P3, Marseille, France

* Deceased